Flash point prediction with UNIFAC type models of ethylic biodiesel and binary/ternary mixtures of FAEEs

Débora Costa do Nascimento[a], Natália Daniele Dorighello Carareto[b], Antonio Marinho Barbosa Neto[c], Vincent Gerbaud[d], Mariana Conceição da Costa[a,*]

[a] School of Chemical Engineering (FEQ), University of Campinas (UNICAMP), 13083-852, Campinas, Sao Paulo, Brazil
[b] Laboratoire des Matériaux Céramiques et Procédés Associés (LMCPA), Université de Valenciennes et du Hainaut-Cambrésis, Valenciennes, France
[c] ThermoPhase, Department of Petroleum Engineering, Santa Catarina State University, 88336-275, Balneário Camboriú, Santa Catarina, Brazil
[d] Laboratoire de Génie Chimique, Université de Toulouse, CNRS – INP – UPS, Toulouse, France

ARTICLE INFO

Keywords:
Flash point
Ethyl esters
Biodiesel
UNIFAC

ABSTRACT

In order to guarantee safe handling of a combustible liquid, such as biodiesel, it is important to be aware of its Flash Point (FP). Thus, the present study focused on FP experimental measurement and thermodynamic correlation of binary and ternary mixtures of saturated or unsaturated fatty acid ethyl esters (FAEEs) as surrogates for biodiesel. FP of different types of ethylic biodiesel in terms of feedstock (canola, corn, cotton and soy oils) were also measured and compared with the predicted values. Experiments were carried out in agreement with the standard closed cup procedure ASTM D6450. Liaw's model was applied to FP prediction, with liquid phase non-ideality description accounted for by UNIFAC group contribution models (Original UNIFAC, UNIFAC-Dortmund and UNIFAC-Bessa with revised parameters for fats). FP prediction accounting for non-ideality proved to be accurate, with some difference between the UNIFAC type models and Root Mean Square Deviations (RMSD) varying from 0.27 K to 3.95 K for binary and ternary mixtures.

1. Introduction

Safe transportation and stocking of a flammable or combustible substance/solution frequently requires the knowledge of its Flash Point (FP). FP of a liquid substance, or a mixture of substances, is defined as the lowest temperature at which such substances release vapor enough to produce a combustible mixture with air [1].

Since FP data is a crucial parameter to storage, handling and transportation of flammable materials, a series of studies on predicting the FP of pure substances and mixtures can be found in the literature [2–11]. FP has a strong importance related to legal requirements and safety; thus, FP is normally specified to meet insurance and fire regulations. In order to be in accordance with American Society of Testing and Materials guidelines, diesel and biodiesel, for example, must have a minimum FP of 311 K [12] and 360 K [13], respectively.

Biodiesel is defined as the product of a transesterification reaction between a fat source, vegetable oils or animal fats for instance, and a short chain alcohol, frequently methanol or ethanol [14]. Usually, the reaction occurs in the presence of a catalyst, as sodium hydroxide, at elevated temperatures [15]. When ethanol is used for the reaction, the resulting ethylic biodiesel is composed by Fatty Acid Ethyl Esters (FAEE), saturated and/or unsaturated. Today, biodiesel is seen as a real alternative substitute to conventional petroleum diesel because it presents some advantages since it is biodegradable and non-toxic; it also has low carbon content, high lubricity and higher FP compared to diesel [14].

The alkyl ester composition of biodiesel is strictly associated to the feedstock from which it is produced. So the physicochemical properties, including the FP, of biodiesel can have substantial variations depending on the raw material used in its production [16]. Typically, biodiesel produced from coconut oil, which is rich in lauric acid [17], exhibits a FP different from biodiesel produced from palm oil, rich in oleic and palmitic acid [15,16].

Besides FP, there are other properties involved in a complete flammability characterization of biodiesel, such as the vapor pressure, the boiling point, lower and upper flammability limits and the lower heating value [18]. Additionally, not only biodiesel handling itself demands fire hazard evaluation, but the whole biodiesel processing cycle presents flammability concerns, as it involves flammable short chain alcohols, as methanol and ethanol, and dangerous catalysts [18]. In fact, the accident rate in biodiesel production has increased in recent years due to lack of operational experience and standardized

* Corresponding author.
E-mail address: mcdcosta@unicamp.br (M.C. da Costa).

https://doi.org/10.1016/j.fuel.2020.118717

operational procedures, being fire the most frequent scenario in accidents, incidents and mishaps in the industry [19,20]. Additionally, biodiesel is more sensitive to oxidative degradation than conventional diesel due to high oxygen content and presence of double bonds [21]. Moreover, biodiesel oxidation caused by ageing and poor storage might lead to peroxide formation, which makes it more unstable over time [21–23].

Still, there are few works on the literature concerning biodiesel fire hazard through FP evaluation [5,6,24–29]. Despite the need for information on flammability characterization of biodiesel and its production process, the correlation between biodiesel's FP, its composition and its solution behavior through Excess Gibbs Energy in terms of activity coefficient evaluation is rarely studied.

Vapor pressure type models, which combine Le Chatelier's rule to Vapor Liquid Equilibrium (VLE) thermodynamics are known for being able to correlate composition of a given liquid to its FP. These types of models are highly dependent on how the vapor pressure of each component is represented and how the non-ideality of the liquid phase is described. In other words, these models depend on the correlation between vapor pressure and temperature, and the activity coefficient model chosen to characterize the liquid phase non-ideal behavior [30]. One may choose one model from a series of available Gibbs Excess Energy models in order to calculate the activity coefficient of each chemical species involved in a mixture. While dealing with ethylic biodiesel, a mixture of FAEEs, predictive models based on group contributions may be the convenient choice to describe the solution's behavior, but these approaches must be validated first.

Predictive models such as UNIFAC type models have the potential to describe non ideal behavior of liquid solutions for non-electrolytic systems [31,32]. The main advantage of UNIFAC is its wide range of application [33]. Effort has been made to improve the prediction performance of the UNIFAC method [34–37]. Even though other methods (Margules equations, van Laar equation, and NRTL method, among others) exist, they require parameter fitting for each system under study. Instead, the UNIFAC method can be used in a fully predictive manner. Regarding FP predictions, UNIFAC has been extensively used to predict non-ideal solution behavior responsible for the occurrence of minimum or maximum FP behavior in miscible mixtures [38] and partially miscible mixtures [3,39].

With this in mind, the aim of this study is to verify whether and to what extent three UNIFAC type models, namely Original UNIFAC [40], UNIFAC-Dortmund [35,36,41] and UNIFAC-Bessa [34], are capable of describing possible liquid phase non idealities of systems containing FAEEs (saturated and unsaturated), including real biodiesel, in an attempt to accurately predict FP of these systems through a FP mixing rule. Therefore, we wished to verify whether the use of UNIFAC activity coefficient models contribute to the improvement of FP prediction of these systems in comparison to the ideal model. To do so, we characterized the flammability of pure FAEEs, as well as 20 binary and 2 ternary mixtures containing FAEEs (saturated or unsaturated) through the measurement of their FP temperatures in a closed cup apparatus according to ASTM D6450 standard procedure. We also measured the FP of four ethylic biodiesels from different feedstocks (Cotton, Canola, Soy and Corn oils). Then, predicted FP values were compared to experimental data by means of RMSD calculation. Furthermore, as FP prediction through Le Chatelier's rule depends not only on the activity coefficient but also on the Vapor Pressure of each component, we checked whether the choice of vapor pressure model between a group contribution model and Antoine's equation affects FP prediction.

2. Methods and tools

2.1. Material

Saturated FAEEs (Table 1) with a high grade of purity were obtained from Sigma-Aldrich, being used as received, i.e. with no further purification. Unsaturated FAEEs with Technical Grade Purity were also obtained from Sigma-Aldrich. Dodecane (Sigma-Aldrich, purity of 0.99 w/w), which is a FP certified reference material, was used to verify the calibration of the FP tester. Canola, cotton, soy and corn Biodiesel samples were produced by a transesterification reaction using ethanol and sodium ethoxide as a catalyst in the lab. The compositions of these four biodiesel samples were characterized through Gas Chromatography.

Binary and ternary sample mixtures of FAEEs were prepared on an analytical scale (Adam AAA/L) with a ± 0.2 mg accuracy by weighting previously known amounts of each FAEE to cover the entire range of molar fraction obtaining a total sample mass of approximately 4 g.

2.2. Flash point measurements

A Miniflash FLPH Touch® from Grabner Instruments (Austria) was used to perform the FP measurements in accordance with ASTM D6450 standard test method [35] with the set of selected parameters: start of test, 18 K before the expected FP; end of test, 10 K after the expected FP; test interval of 1 K; heating rate of 5.5 K/min; and pressure threshold for the flash detection of 20 kPa. The values are discussed in Section 3.1.

The ASTM D6450 FP detection method consists in measuring the instantaneous pressure increase inside the closed chamber triggered by an energy-controlled electric arc. The ambient pressure was checked every day in order to correct the measured flash point to a pressure of 101.3 kPa. A test specimen of 1 mL was used in each measurement, as recommended by the standard method, and its homogeneity was ensured by a magnetic stirrer. Moreover, the flash point tester performance was evaluated every day with dodecane (FP = 352.2 ± 2.1 K). All the analysis were performed in triplicate, always using a fresh test specimen, and the average FP value was calculated.

2.3. Flash point model

A Vapor Pressure based mathematical approach can be used to describe the flash point of miscible mixtures [1,43]. One can find an extensive discussion on this approach on the literature [1,11,16,28,43,44]. The equation that describes FP for multi component mixtures is equal to

$$1 = \sum_{i=1}^{n} \frac{x_i \gamma_i P_i^{sat}}{P_{i,FP}^{sat}} \quad (1)$$

where n represents the total of flammable substances in the mixture, x_i is the molar fraction of i in the liquid phase, γ_i is liquid phase activity coefficient of i, P_i^{sat} is the vapor pressure of pure component i in Pa at the FP temperature of the mixture and, $P_{i,FP}^{sat}$ is the vapor pressure of pure component i in Pa at its FP temperature. In this equation, the vapor pressures and activity coefficients of each pure component are a function of the FP temperature of the mixture.

We used three variants of the UNIFAC model to calculate the activity coefficients of the mixtures needed in Eq. (1): UNIFAC original [40], UNIFAC-Dortmund [35,36,41] and a readjusted UNIFAC for biodiesel mixtures [34] – here named UNIFAC-Bessa. While Dortmund considers a temperature dependency of interaction parameters, Bessa suggests a specific set of parameters regressed from fats equilibrium data.

In order to evaluate the dependence of Eq. (1) on the vapor pressure, saturated FAEE vapor pressures were calculated by two different methods:

- Method 1: the FAEE vapor pressure is computed by using the group contribution model proposed by Ceriani et al. [45].
- Method 2: the FAEE vapor pressure is computed from Antoine's equation.

Table 1
Flash point of the pure FAEE used in this work.

FAEE (CAS number)	Purity[a] (w/w)	Flash point (K)					
		Catoire model[b]	ASTM D6450[c]	ASTM D93C[d]	ΔFP		
					(ASTM D6450 – ASTM D93C)	(ASTM D6450 – Catoire)	(ASTM D93C – Catoire)
Ethyl Octanoate (106-32-1)	0.997	353.2	354.0 ± 0.1	360.8	−6.8	0.8	7.6
Ethyl Decanoate (110-38-3)	0.996	378.7	379.5 ± 0.6	387.7	−8.2	0.8	9.0
Ethyl Laurate (106-33-2)	0.997	400.6	402.3 ± 0.6	399.7	2.6	1.7	−0.9
Ethyl Myristate (124-06-1)	0.991	425.3	423.6 ± 0.6	423.7	−0.1	−1.7	−1.6
Ethyl Pentadecanoate (41114-00-5)	0.983	–	432.0 ± 1.0	–	–	–	–
Ethyl Palmitate (628-97-7)	0.995	442.5	443.2 ± 0.6	433.8	9.4	0.7	−8.7
Ethyl Stearate (111-61-5)	0.992	457.2	458.3 ± 0.6	464	−5.7	1.1	6.8
Ethyl Oleate (111-62-6)	Technical Grade	458.0	453.1 ± 0.6	427	26.2	−4.9	−31.0
	0.980		457.7 ± 0.6	–	–	-0.3	–
Ethyl Linoleate (544-35-4)	Technical Grade	453.0	455.2 ± 0.6	429	26.2	2.2	−24.0

[a] According to the supplier.
[b] Calculated from Catoire's model [42].
[c] This work ± standard deviation.
[d] From [16].

Ceriani's equation (Eq. (2)) is a group contribution based method for vapor pressure prediction of substances found in fats and oils, such as fatty esters, fatty acids and acylglycerols. It was chosen to be tested along with Antoine's law due to its predictive character. It also has been validated in the literature for fatty esters and acids [28,46,47], and, differently from Antoine's law, its range of applicability is not strictly limited by temperature or vapor pressure data availability.

$$\ln(P_i^{sat}) = A_i + \frac{B_i}{T} + C_i \cdot \ln(T) \quad (2)$$

Ceriani's equation parameters A_i, $B_i$and C_i are calculated from the expressions:

$$A_i = \sum_k N_k \cdot (A_{1k} + M_i \cdot A_{2k}) + (s_0 + N_{cs} \cdot s_1) + \alpha \cdot (f_0 + N_c \cdot f_1) \quad (3)$$

$$B_i = \sum_k N_k \cdot (B_{1k} + M_i \cdot B_{2k}) + \beta \cdot (f_0 + N_c \cdot f_1) \quad (4)$$

$$C_i = \sum_k N_k \cdot (C_{1k} + M_i \cdot C_{2k}) \quad (5)$$

where the index k refers to the types of groups found in the molecule, which can be CH_3, CH_2, COOH, C=, OH, COO, and CH_2-$CHCH_2$. A_{1k}, B_{1k}, C_{1k}, A_{2k}, B_{2k}, C_{2k}, α, β, s_0, s_1, f_0 and f_1 are parameters adjusted from an extensive vapor pressure database of fats and oils. M_i is the molar mass of component i, N_c is the number of carbons in the molecule, and N_{cs} is the number of carbon atoms in the alcoholic part of the fatty ester, which is 2 for ethyl esters.

Thus, we will use and compare both methods in this work. Antoine parameters were used to describe the vapor pressure of ethyl octanoate, ethyl decanoate, ethyl laurate and, ethyl myristate [48]. Antoine's coefficients A_i, B_i and C_i of each FAEE are listed in Table 2. However, no Antoine parameters were found in the temperature range of interest for ethyl palmitate and ethyl stearate. Therefore, for these two FAEEs the group contribution model (Method 1) was used.

Table 2
Antoine equation parameters to some FAEE (P_i^{sat} in Pa and T in K).

FAEE	Temperature range/K	A_i	B_i	C_i
Ethyl Octanoate	283.8 to 462.31	9.385	1766	−78.15
Ethyl Decanoate	313.1 to 462.37	9.85	2169	−67.45
Ethyl Laurate	303.1 to 462.43	10.738	2894	−36.95
Ethyl Myristate	333.22 to 462.3	10.153	2571	−75.55

$$\log_{10} P_i^{sat} = A_i - \frac{B_i}{T + C_i} \quad (6)$$

The root mean square deviation (*RMSD*) between experimental data and predicted values is calculated according to Eq. (7).

$$RMSD = \sqrt{\sum_{k=1}^{m} \left(\frac{(T_{FP,k}^{exp} - T_{Fp,k}^{mod})^2}{m} \right)} \quad (7)$$

where $T_{FP,k}^{exp}$ is the average of measured FP in K at point k, $T_{FP,k}^{mod}$ is the FP temperature predicted by the model in K at point k, and m is the number of experimental points.

3. Results and discussion

3.1. Flash point of pure saturated FAEEs

Pure FAEEs FP values measured by means of the ASTM D6450 method are listed in Table 1. The standard deviations of experimental measurements were estimated by performing repeated experimental runs at least three times with each pure FAEE. These deviations stayed in the range of 0.06 to 1 K. The variation coefficients of these measurements are within the range of 0.1 – 0.6 %. These values are lower than those observed for FP data already reported in the literature [11,49,50].

As it can be seen in Fig. 1, the FP of pure even-numbered FAEEs increases almost linearly as a function of the carbon length. This behavior is strongly related to the volatility of the fatty substances and

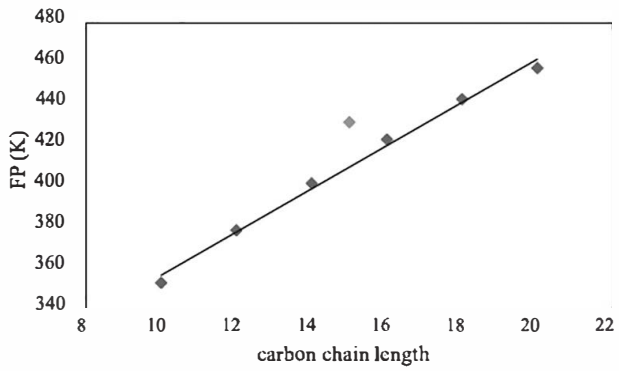

Fig. 1. Flash point of FAEEs as a function of their carbon chain length. (—) is the linear regression corresponding to the FP of the even-numbered FAEEs.

Table 3
FP results for the Saturated FAEEs binary systems.

ethyl octanoate + ethyl laurate			*ethyl decanoate + ethyl myristate*			*ethyl laurate + ethyl palmitate*		
$x_{ethyl\ octanoate}$	FP/K	SD	$x_{ethyl\ decanoate}$	FP/K	SD	$x_{ethyl\ laurate}$	FP/K	SD
0.0000	402.3	0.6	0.0000	423.6	0.6	0.0000	443.2	0.6
0.1077	390.4	0.6	0.0993	412.8	0.1	0.1041	433.9	0.1
0.1978	381.5	0.6	0.2075	403.9	0.1	0.2008	427.9	0.1
0.4015	371.0	0.1	0.4019	395.8	0.1	0.4042	418.5	0.6
0.6011	364.0	0.1	0.5974	388.7	1.0	0.6023	412.9	0.1
0.7967	359.0	0.1	0.8006	384.9	0.1	0.7981	407.9	0.1
1.0000	354.0	0.1	1.0000	379.5	0.6	1.0000	402.3	0.6
ethyl octanoate + ethyl myristate			*ethyl decanoate + ethyl palmitate*			*ethyl laurate + ethyl stearate*		
$x_{ethyl\ octanoate}$	FP/K	SD	$x_{ethyl\ decanoate}$	FP/K	SD	$x_{ethyl\ laurate}$	FP/K	SD
0.0000	423.6	0.6	0.0000	443.2	0.6	0.0000	458.3	0.6
0.1031	399.0	0.1	0.1155	419.5	0.5	0.1268	439.3	0.6
0.2051	386.3	0.6	0.2056	411.7	0.1	0.2148	432.1	0.6
0.4022	372.6	0.6	0.4172	397.7	0.1	0.4006	420.4	0.6
0.6002	365.0	0.1	0.5993	390.7	0.1	0.5970	413.8	0.1
0.7988	359.3	0.6	0.7997	385.8	0.1	0.7924	408.3	0.6
1.0000	354.0	0.1	1.0000	379.5	0.6	1.0000	402.3	0.6
ethyl octanoate + ethyl palmitate			*ethyl decanoate + ethyl stearate*			*ethyl myristate + ethyl palmitate*		
$x_{ethyl\ octanoate}$	FP/K	SD	$x_{ethyl\ decanoate}$	FP/K	SD	$x_{ethyl\ myristate}$	FP/K	SD
0.0000	443.2	0.6	0.0000	458.3	0.6	0.0000	443.2	0.6
0.1224	401.0	1.7	0.0948	430.6	0.6	0.1028	439.9	1.0
0.2272	385.0	0.1	0.1994	414.3	0.6	0.2013	437.9	0.1
0.3995	373.3	0.6	0.4013	397.3	0.6	0.3982	433.2	0.6
0.6004	365.6	0.6	0.5826	391.1	0.2	0.5992	429.9	0.1
0.8096	359.0	0.1	0.7970	385.0	0.1	0.7995	426.5	0.6
1.0000	354.0	0.1	1.0000	379.5	0.6	1.0000	423.6	0.6
ethyl octanoate + ethyl stearate			*ethyl laurate + ethyl myristate*			*ethyl myristate + ethyl stearate*		
$x_{ethyl\ octanoate}$	FP/K	SD	$x_{ethyl\ laurate}$	FP/K	SD	$x_{ethyl\ myristate}$	FP/K	SD
0.0000	458.3	0.6	0.0000	423.6	0.6	0.0000	458.3	0.6
0.1009	407.6	0.6	0.1010	420.8	0.1	0.1836	447.4	0.6
0.2025	390.0	0.1	0.2020	417.8	0.1	0.2629	443.8	0.1
0.4030	374.0	0.1	0.4037	412.8	0.1	0.4020	438.8	0.1
0.5866	366.0	0.1	0.6002	409.1	0.6	0.6424	430.9	0.1
0.7997	360.0	0.1	0.7981	405.9	0.1	0.8141	427.5	0.6
1.0000	354.0	0.1	1.0000	402.3	0.6	1.0000	423.6	0.6

consequently to their boiling point. In other words, the higher the carbon chain, the lower the volatility. Lower volatility for flammable substances implies a higher FP. We recall that Catoire's empirical model for predicting the FP of pure compounds and blends correlates FP with the boiling temperature and carbon chain [42,51,52]. Catoire's model relies on a large FP dataset of organic compounds and has been proven to be quite accurate for FP prediction of pure substances [42]. In this study, FPs of pure FAEEs were calculated from Catoire's model (Table 1), with normal boiling points and number of carbons described on Table S1 of the supplementary material. As Table 1 shows, FPs obtained from ASTM D6450 are way closer to values predicted from Catoire's model than FPs obtained from ASTM D93C are. Differences between calculated and experimental FP are lower than 4.9 K for ASTM D6450, while for ASTM D93C the difference can be of up to 30 K. This observation, among other circumstances, led us to choose ASTM D6450 instead of ASTM D93C.

Another factor we considered for choosing ASTM D6450 over ASTM D93C was linear character of FP as a function of chain size. The outlier point in Fig. 1 refers to ethyl pentadecanoate. This behavior is explained by the odd-numbered carbon chain length of ethyl pentadecanoate. Normally, some properties, such as melting point, density, enthalpy of vaporization and normal boiling point, increase linearly for even-numbered carbon chain substances, as fatty acids, fatty acid alkyl esters and dicarboxylic acids [48,53–56]. Odd-numbered carbon chain fatty substances also present another linear increase for physicochemical properties with a different expression from the even-numbered carbon chain linear dependency [48,53–56]. We expect that such behavior can be observed to FP too.

Since the FP of even-numbered FAEEs had been measured in a previous study using the ASTM D93C method, we also listed these resulting values in Table 1. The difference between the values ranges from 0.1 to 9.4 K. According to ASTM, the reproducibilities (R) of ASTM D6450 and ASTM D93C methods are equal to R = 3.1 K and R = 14.7 K [57,58], respectively. Based on that, we can consider that pure saturated FAEEs FPs are in agreement with each other. Besides, the ASTM D6450 FPs displayed in Fig. 1 can be regressed linearly versus the carbon chain length for the even-numbered FAEEs with $R^2 = 0.9934$, whereas for the ASTM D93C FP data set in Table 1, the correlation as a function of carbon chain length is equal to $R^2 = 0.9843$. This implies that the new set of data measured by the ASTM D6450 is more linearly consistent than the ASTM D93C data set.

Another reason behind choosing ASTM D6540 over ASTM D93 is that ASTM D6450 provides a more controlled environment for FP measurement, as it demands smaller sample volumes and guarantees continuous agitation during the measurements, allowing uniform vapor–liquid phase temperature, which has equilibrium implications, even though both methods are dynamic, and relies on controlled air injection to provide oxygen for combustion.

In addition to showing a better consistency in FP values for the even-numbered FAEEs, ASTM D6450, again, presents the advantage of using only 1 mL of sample in each analysis. This can reduce drastically the cost of measurements in contrast to the ASTM D93C method, which requires 75 mL.

3.2. Flash point of pure unsaturated FAEEs

FPs of Ethyl Oleate and Ethyl Linoleate were measured as well (Table 1). The standard deviations of these measurements were about 0.6 K, with variation coefficients lower than 0.2%. Table 1 shows that the FP values of these FAEEs were lower than the FP of Ethyl Stearate. As observed in a previous work, the FP of FAEEs depends on carbon chain size and number of unsaturation [16]. Therefore, even though Ethyl Oleate and Ethyl Linoleate have the same carbon chain size as Ethyl Stearate, the presence of any unsaturation causes the vapor pressure to increase, which reduces the FP consequently.

There is some discrepancy between experimental data obtained through the standard Method ASTM D6450 and the values obtained by ASTM D93 measurements. This could be due to the fact that the purities of the unsaturated FAEEs used in this study and the ones in the literature were not high, Technical Grade (TG), which implies that contaminants, such as ethyl palmitate (C16:0) and ethyl stearate (C18:0) were present in a variety of considerable concentrations. In fact, the TG ethyl oleate and TG ethyl linoleate used in this study do contain ethyl palmitate and ethyl stearate. Characterization of these reagents through gas chromatography indicated TG ethyl oleate's molar composition to be 1.91% ethyl stearate, 88.39% ethyl oleate and 9.70% ethyl linoleate, while TG ethyl linoleate's molar composition is made of 7.98% ethyl palmitate, 2.26% ethyl stearate, 12.66% ethyl oleate and 77.10% ethyl linoleate.

3.3. Flash point of binary and ternary mixtures

Experimental FP values of the binary mixtures involving saturated esters are presented in Table 3 and plotted in Fig. 2. FP values of the ternary mixtures of saturated FAEEs are presented in Table 4 and represented in Fig. 3. These sets of data show standard deviations comparable to those observed for pure FAEEs, ranging from 0.01 to 1.0 K, and variation coefficients within the range of 0.0–0.2 %. Additionally, experimental data on binary systems containing unsaturated FAEEs + saturated FAEEs are presented in Table 5 (Ethyl Oleate + Saturated FAEE) and Table 6 (Ethyl Linoleate + Saturated FAEE). The standard deviation for these sets of data range from 0.1 to 3.1 K, while the variation coefficients are lower than 0.7% in general.

$$SD = \sqrt[2]{\frac{\sum_{k=1}^{3} (FP_k - \overline{FP})^2}{3}}$$

where $\overline{FP}$ is the average FP, FP_k is one of the measured FP values out of three measurements.

3.3.1. FP modeling method 1 for saturated FAEEs

FP of binary and ternary mixtures of Saturated FAEEs were calculated by using Ceriani's group contribution method [45] for vapor pressure and testing three UNIFAC type models (Original, Dortmund and Bessa) to estimate activity coefficients of components in the liquid phase. Detailed results are presented as Supplementary Data, as well as results obtained assuming an ideal behavior for the liquid phase ($\gamma_i = 1$).

The Root Mean Square Deviation (*RMSD*) between experimental data and predicted values are exposed in Table 7. These values show that the FP temperature predicted from the activity coefficient models are in agreement with the experimental data. *RMSD* values range from 0.27 K to 3.54 K. Overall, the UNIFAC Bessa model showed better results, with a *RMSD* between 0.27 and 1.47 K. In detail, we can note that while the lowest deviation is found for the system formed by ethyl myristate + ethyl palmitate (*RMSD* from 0.27 to 0.28 K), the highest deviation is found for the system containing ethyl octanoate + ethyl stearate (*RMSD* from 1.47 to 3.54 K).

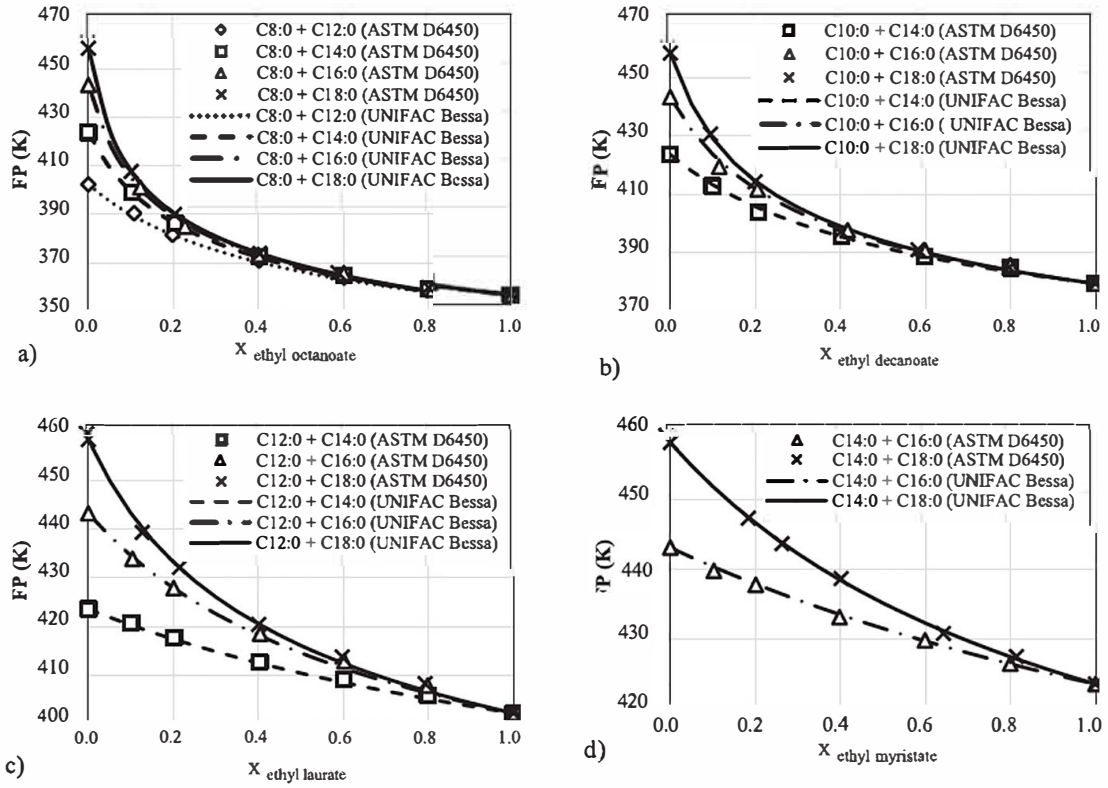

Fig. 2. FP experimental and predicted values (UNIFAC Bessa/Method 2) of Saturated FAEE binary mixtures.

Table 4
FP results for the Saturated FAEES ternary systems.

ethyl decanoate + ethyl myristate + ethyl stearate					*ethyl laurate + ethyl myristate + ethyl palmitate*				
$x_{ethyl\ decanoate}$	$x_{ethyl\ myristate}$	$x_{ethyl\ stearate}$	FP/K	SD	$x_{ethyl\ laurate}$	$x_{ethyl\ myristate}$	$x_{ethyl\ palmitate}$	FP/K	SD
0.7689	0.1114	0.1198	384.8	0.1	0.7987	0.0984	0.1029	406.4	0.6
0.5495	0.1064	0.3441	390.5	0.6	0.5979	0.1007	0.3013	411.4	0.6
0.4024	0.1029	0.4947	395.2	0.6	0.4471	0.1074	0.4455	415.8	0.1
0.2607	0.0966	0.6427	404.2	0.6	0.3007	0.1032	0.5961	421.8	0.1
0.0806	0.0987	0.8207	426.9	0.1	0.1010	0.1051	0.7939	432.1	0.6
0.5583	0.3219	0.1198	389.9	0.1	0.6005	0.2992	0.1003	410.1	0.6
0.4084	0.4760	0.1156	393.5	0.6	0.4494	0.4500	0.1006	412.8	0.1
0.2735	0.6143	0.1122	400.5	0.6	0.3032	0.5975	0.0993	416.8	0.1
0.0893	0.8032	0.1075	414.5	0.6	0.1018	0.7960	0.1022	421.8	0.1
0.0816	0.2854	0.6330	422.9	0.1	0.1045	0.2993	0.5963	428.5	0.6
0.0839	0.4365	0.4796	420.2	0.6	0.1006	0.4508	0.4486	426.9	0.1
0.0885	0.5865	0.3251	416.9	0.1	0.0999	0.6001	0.3000	424.5	0.6
0.5099	0.2615	0.2287	390.9	0.1	0.5488	0.2476	0.2036	411.9	0.1
0.3561	0.2516	0.3923	397.5	0.6	0.4035	0.2490	0.3476	415.9	0.1
0.2137	0.2473	0.5390	407.5	0.6	0.2493	0.2502	0.5005	421.5	0.6
0.3602	0.3588	0.2810	397.2	0.6	0.3801	0.3651	0.2548	415.1	0.6
0.2196	0.5057	0.2747	405.2	0.6	0.2524	0.4980	0.2496	418.8	0.1
0.2182	0.3473	0.4345	406.2	0.6	0.2531	0.3488	0.3981	420.8	0.1
0.2585	0.3595	0.3821	402.9	0.1	0.3335	0.3311	0.3354	417.8	0.1

SD stands for Standard Deviation.

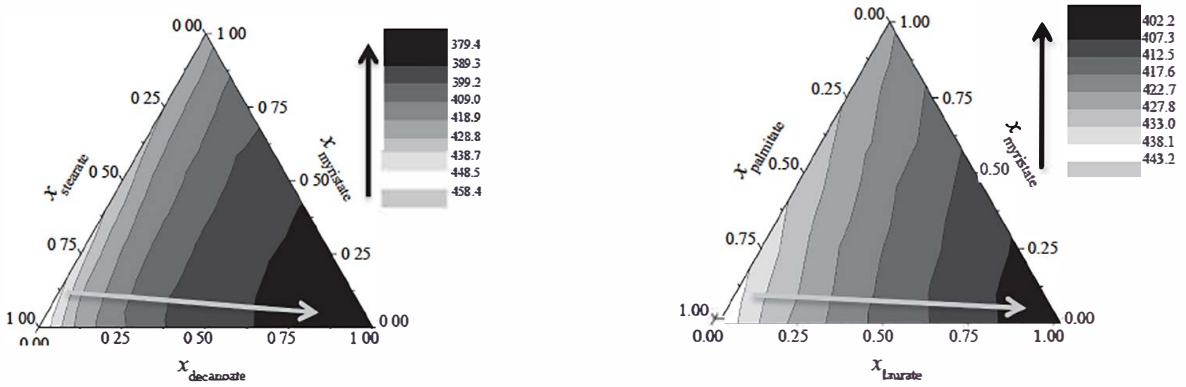

Fig. 3. FP experimental values of ternary mixtures. a) ethyl decanoate + ethyl myristate + ethyl stearate; b) ethyl laurate + ethyl myristate + ethyl palmitate.

Table 5
FP results for Ethyl Oleate + saturated FAEEs binary systems.

ethyl octanoate + ethyl oleate			*ethyl decanoate + ethyl oleate*		
$x_{ethyl\ octanoate}$	FP/K	SD	$x_{ethyl\ decanoate}$	FP/K	SD
0.0	453.1	0.6	0.0	453.1	0.6
0.1	406.4	0.6	0.1	426.9	0.1
0.2	388.8	1.0	0.2	413.9	0.1
0.4	374.1	0.6	0.4	398.5	0.6
0.6	364.8	0.1	0.6	390.2	0.6
0.8	359.8	0.1	0.8	384.8	0.1
1.0	354.0	0.1	1.0	379.5	0.6
ethyl laurate + ethyl oleate			*ethyl myristate + ethyl oleate*		
$x_{ethyl\ laurate}$	FP/K	SD	$x_{ethyl\ myristate}$	FP/K	SD
0.0	453.1	0.6	0.0	453.1	0.6
0.1	440.1	0.6	0.1	448.1	0.6
0.2	430.8	0.1	0.2	443.4	0.6
0.4	419.9	0.1	0.4	437.4	3.1
0.6	412.5	0.6	0.6	430.8	1.0
0.8	407.2	0.6	0.8	426.1	0.6
1.0	402.3	0.6	1.0	423.6	0.6

Table 6
FP results for Ethyl Linoleate + saturated FAEEs binary systems.

ethyl octanoate + ethyl linoleate			*ethyl decanoate + ethyl linoleate*		
$x_{ethyl\ octanoate}$	FP/K	SD	$x_{ethyl\ decanoate}$	FP/K	SD
0.0	455.2	1.6	0.0	455.2	1.6
0.1	407.8	0.1	0.1	426.0	0.6
0.2	391.1	0.6	0.2	414.0	0.6
0.4	374.4	0.6	0.4	399.1	0.6
0.6	365.8	0.1	0.6	390.8	0.1
0.8	360.8	0.1	0.8	384.4	0.6
1.0	354.0	0.1	1.0	379.5	0.6
ethyl laurate + ethyl linoleate			*ethyl myristate + ethyl linoleate*		
$x_{ethyl\ laurate}$	FP/K	SD	$x_{ethyl\ myristate}$	FP/K	SD
0.0	455.2	1.6	0.0	455.2	1.6
0.1	441.8	0.1	0.1	448.5	0.6
0.2	432.1	0.6	0.2	444.5	0.6
0.4	420.4	0.6	0.4	437.9	0.1
0.6	412.7	0.1	0.6	431.8	0.1
0.8	407.7	0.1	0.8	427.8	0.1
1.0	402.3	0.6	1.0	423.6	0.6

Table 7
RMSD between the experimental data and the predicted values from ideal curve, UNIFAC Original, UNIFAC Dortmund and UNIFAC Bessa and vapor pressure calculated with Method 1 and Method 2.

System	*RMSD*/K							
	Method 1				Method 2			
	Ideal	UNIFAC Original	UNIFAC Dortmund	UNIFAC Bessa	Ideal	UNIFAC Original	UNIFAC Dortmund	UNIFAC Bessa
Ethyl octanoate + ethyl laurate	1.36	1.23	1.38	1.08	1.11	1.52	1.13	0.86
Ethyl octanoate + ethyl myristate	1.83	1.45	1.84	1.07	1.24	0.96	1.26	0.64
Ethyl octanoate + ethyl palmitate	2.53	1.86	2.51	1.29	1.16	1.05	1.58	0.91
Ethyl octanoate + ethyl stearate	3.54	2.41	3.42	1.47	2.39	1.29	2.28	0.75
Ethyl decanoate + ethyl myristate	0.86	0.87	0.87	0.88	0.86	0.91	0.87	0.95
Ethyl decanoate + ethyl palmitate	1.78	1.59	1.77	1.45	1.33	1.30	1.34	1.32
Ethyl decanoate + ethyl stearate	2.26	1.70	2.14	1.36	1.26	0.90	1.14	0.91
Ethyl laurate + ethyl myristate	0.61	0.61	0.62	0.59	0.54	0.52	0.54	0.51
Ethyl laurate + ethyl palmitate	1.43	1.36	1.42	1.31	1.03	0.99	1.03	0.97
Ethyl laurate + ethyl stearate	1.57	1.38	1.52	1.27	0.99	0.93	0.98	0.93
Ethyl myristate + ethyl palmitate	0.28	0.27	0.28	0.27	0.29	0.29	0.29	0.31
Ethyl myristate + ethyl stearate	0.78	0.71	0.76	0.67	0.29	0.27	0.28	0.27
Ethyl laurate + ethyl myristate + ethyl palmitate	0.93	0.88	0.92	0.84	0.6	0.56	0.59	0.53
Ethyl decanoate + ethyl myristate + ethyl stearate	0.78	1.10	0.81	1.38	1.48	1.88	1.55	2.18
RMSD Max	3.54	2.41	3.42	1.47	2.39	1.88	2.28	2.18
RMSD Min	0.28	0.27	0.28	0.27	0.29	0.27	0.28	0.27

[a] The vapor pressure for ethyl palmitate and ethyl stearate were calculated with the group contribution model proposed by [45].

3.3.2. FP modeling method 2 for saturated FAEEs

FP curves calculated using Antoine's law for the vapor pressures of Saturated FAEEs and using the three UNIFAC models or the ideal behavior ($\gamma_i = 1$) for the liquid phase are also presented as Supplementary Data. The *RMSD* between experimental data and thermodynamic calculations is presented in Table 7, ranging from 0.27 to 2.39 K. In a similar way as to Method 1, the UNIFAC Bessa model exhibited the best results (*RMSD* from 0.27 to 2.18 K) (Fig. 2). Here, the system ethyl myristate + ethyl stearate showed the lowest deviation with *RMSD* ranging from 0.27 to 0.29 K. The highest deviations are found using UNIFAC Dortmund and the ideal model for ethyl octanoate + ethyl stearate system (*RMSD* equal to 2.28 and 2.39 K, respectively). However, the highest deviations for the UNIFAC original and UNIFAC Bessa models are obtained for the ternary system ethyl decanoate + ethyl myristate + ethyl stearate (*RMSD* equal to 1.18 and 2.18 K, respectively).

3.3.3. Comparison between methods 1 and 2 used to calculate the vapor pressure of saturated FAEEs

Overall, Method 2, which includes a predictive activity coefficient model and Antoine's equation, provided better results than the entirely predictive Method 1. The exception is the ternary system ethyl decanoate + ethyl myristate + ethyl stearate where the use of Method 2 to calculate the FAEEs vapor pressure increased the *RMSD* from an average value of 1.02 K to 1.77 K.

Antoine coefficients were obtained from the literature. No extrapolation was needed in order to apply Antoine's equation to vapor pressure calculation for the systems under study, which implies that this may be an accurate vapor pressure model depending on the reliability of the vapor pressure data that it was adjusted to. As Ceriani's model is a predictive approach to vapor pressure calculation based on group contributions, we expected that its influence on FP calculation could become a source of error. Also, Antoine's law, shows better accuracy in comparison to Ceriani's equation, which underestimates vapor pressure values, as shown by Fig. 4. As the FP prediction results suggest, Method 2 was more accurate than Method 1, as expected (Table 7). However, we noticed that *RMSD*s obtained through Method 1 were comparable to Method's 2 *RMSD*s. Therefore, we can conclude that FP prediction is not influenced by the selection of the vapor pressure method (Method 1 or 2). This is advantageous especially when no experimental data on vapor pressure is available, since Method 1 relies on group contribution.

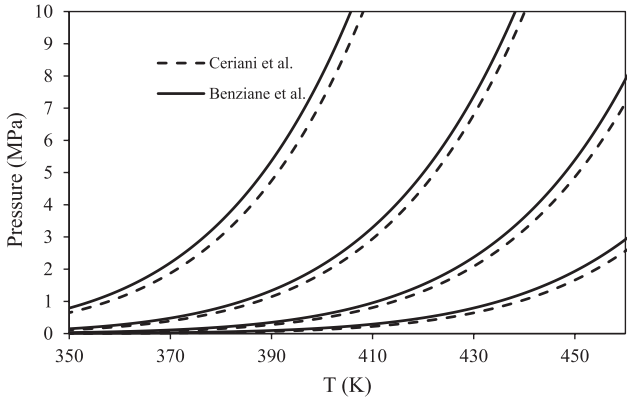

Fig. 4. Vapor pressure values of the FAEEs using the group contribuition method proposed by Ceriani et al. [45] and using the Antoine equation proposed by Benziane et al. [48]. From bottom to top: ethyl myristate, ethyl laurate, ethyl decanoate and ethyl octanoate curves.

3.3.4. Activity coefficients considering binary saturated FAEEs systems

In a previous work [16], in order to estimate the FP of ethylic biodiesel, we assumed that interactions between FAEE molecules were nearly ideal, with $\gamma_i = 1$. This assumption was made based on the chemical structures of these molecules, which can be quite similar, depending mostly on chain size for saturated FAEEs. Therefore, for binary mixtures, as carbon chains become closer in size, we expect a solution behavior closer to the ideality.

In this study, we observed that most binary mixtures containing saturated FAEE molecules present a behavior nearly ideal indeed, which is reflected on FP calculation. As shown in Table 3, RMSDs between experimental and calculated FP considering the ideal model present values close to those obtained through UNIFAC type models. This observation is valid specially when mixture constituents have similar chain sizes. However, as chain sizes diverge, the FP calculated through the ideal model becomes less accurate. For mixtures containing ethyl octanoate, for example, the RMSDs obtained considering the ideal model increase proportionally to carbon chain size divergence. It varies

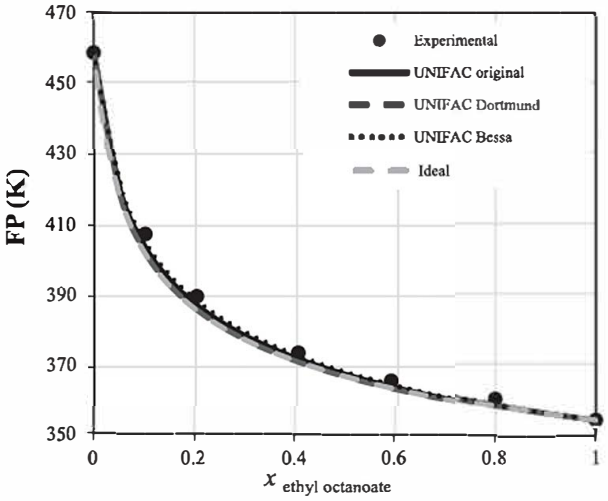

Fig. 5. Comparison between experimental FP and UNIFAC models or ideal curve of binary system ethyl octanoate + ethyl stearate (with vapor pressure calculated using the Method 1).

from an RMSD value of 1.36 K (Method 1) regarding the system ethyl octanoate + ethyl laurate to an RMSD of 3.54 K (Method 1) for ethyl octanoate + ethyl stearate which translates to an absolute discrepancy of up to 5.7 K for this system (Fig. 5).

This maximum absolute discrepancy can be reduced to 2.2 K (1.47 K in terms of *RMSD* for Method 1) by employing the UNIFAC Bessa model to activity coefficient calculation. This suggests that for this system (ethyl octanoate + ethyl stearate), the evaluation of liquid phase non ideality through activity coefficients is important. It should be noticed that from the UNIFAC models tested, UNIFAC Bessa showed the best accuracy in FP prediction concerning most systems, while original UNIFAC came in second, and UNIFAC Dortmund was the least accurate.

The activity coefficients calculated through each of these UNIFAC type models for most FAEE systems are in fact close to unit. For the system containing quite similar molecules, ethyl laurate + ethyl myristate, activity coefficients vary from 0.992 to 1.000 (Fig. 6a and b). In this case the ideal model can be adequate and using an activity coefficient model is not improving significantly the prediction. When it comes to the system ethyl octanoate + ethyl stearate though, activity coefficients calculated by each UNIFAC model vary from 0.75 to 1.05 (Fig. 6c and d), hinting to a non ideal solution behavior, and validating the need for using a model with activity coefficient models. As known from theory, positive deviations from ideality (repulsive interactions between molecules) result in activity coefficients greater than unit, while negative deviations (attractive interactions) result in activity coefficients lower than one. Therefore, the system composed by ethyl octanoate + ethyl stearate deviates negatively from ideality, which means that the vapor pressure of this system is lower than what would be expected from an ideal behavior. This results on the mixture's predicted FP based on the ideal model being lower than the experimental value (Fig. 5). Among the UNIFAC models tested, UNIFAC Bessa was the one able to account for this behavior, whilst original UNIFAC predicted a nearly ideal behavior and UNIFAC Dortmund suggested both attractive and repulsive interactions.

We would like to emphasize that although many of the systems studied are nearly ideal, the UNIFAC models tested, especially UNIFAC Bessa, were still capable of improving FP prediction for most of those systems, as Table 7 shows. This improvement was even more perceptible for systems where the chain sizes of components diverge by more than 4 carbons. Regarding the ternary systems studied, a nearly ideal behavior was observed, which is related to similarity between the molecules involved in the solution.

These results differ in a certain way from what had been observed previously for binary systems containing Fatty Acid Methyl Esters (FAME) [28]. These types of systems seem to behave in an even more ideal way than systems composed by FAEEs. This might be due to structural differences, since FAEEs have a extra carbon atom when compared to FAME in the alcoholic moiety of the molecule. Due to this, UNIFAC type models are not able to improve the FP prediction of solutions formed by FAMEs, while for those containing FAEEs, the improvement is evident.

3.4. FP modelling method 1 for unsaturated FAEEs and activity coefficients

To our best knowledge, there are no Antoine coefficients for unsaturated FAEEs in the literature on the temperature ranges of interest

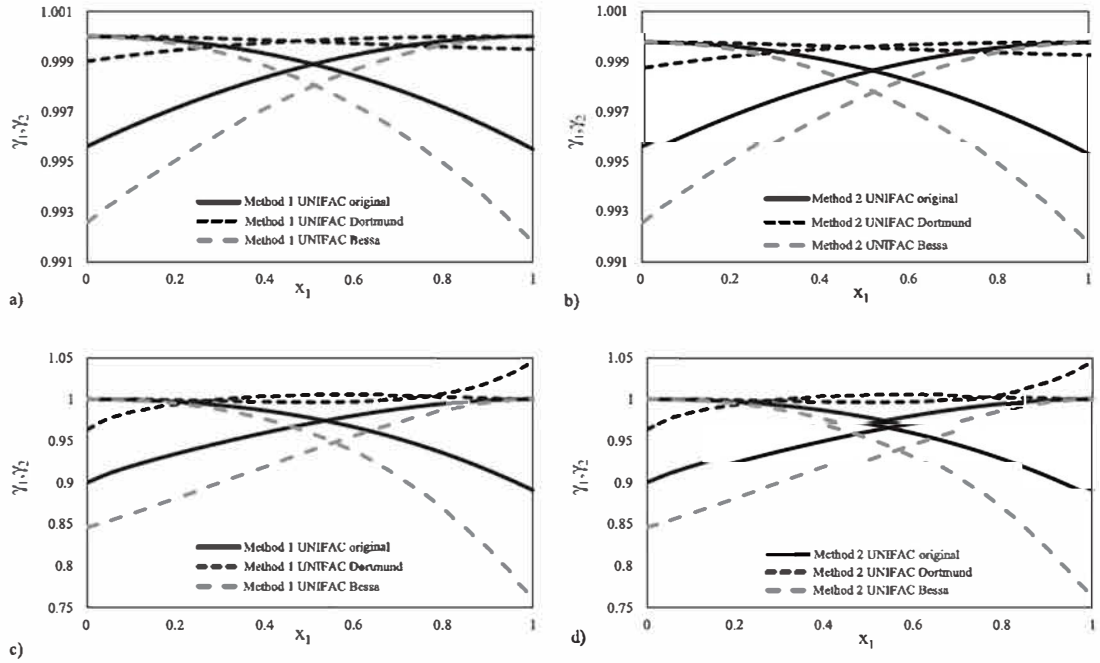

Fig. 6. Activity coefficient of binary systems a) and b) ethyl laurate + ethyl myristate; c) and d) ethyl octanoate + ethyl stearate.

Table 8
RMSD between the experimental data and the predicted values from ideal curve, UNIFAC Original, UNIFAC Dortmund and UNIFAC Bessa and vapor pressure calculated with Method 1 for binary systems containing Unsaturated FAEEs + Saturated FAEEs.

System	*RMSD*/K			
	Method 1			
	Ideal	UNIFAC Original	UNIFAC Dortmund	UNIFAC Bessa
ethyl octanoate + ethyl oleate	2.95	1.69	2.79	1.02
ethyl decanoate + ethyl oleate	1.75	1.07	1.56	0.43
ethyl laurate + ethyl oleate	0.85	0.65	0.78	0.53
ethyl myristate + ethyl oleate	0.68	0.65	0.66	0.66
ethyl octanoate + ethyl linoleate	3.95	2.64	3.78	1.10
ethyl decanoate + ethyl linoleate	2.34	1.64	2.13	0.65
ethyl laurate + ethyl linoleate	1.33	1.08	1.24	0.82
ethyl myristate + ethyl linoleate	0.56	0.48	0.51	0.60
RMSD Max	3.95	2.64	3.78	1.02
RMSD Min	0.56	0.48	0.51	0.43

for this study. As there was no significant difference between Method 1 and Method 2 in terms of FP prediction, Method 1 was selected for the prediction of FP of binary mixtures involving Unsaturated FAEEs.

Overall, UNIFAC type models could improve FP prediction for mixtures containing Unsaturated FAEEs (Table 8). Ethyl linoleate systems seemed to be less ideal than ethyl oleate ones. One can conclude that the presence of double bonds increases the non-ideality of mixtures of saturated esters and unsaturated esters proportionally to the number of double bonds present and how those influence the shape of the unsaturated molecules.

As Table 8 shows, among the three UNIFAC type models used for non-ideality characterization, UNIFAC Bessa resulted in more accurate FP prediction (max. RMSD 1.02 K and min. RMSD 0.43 K). The accuracy in FP prediction with UNIFAC Bessa is similar for systems containing either ethyl oleate and ethyl linoleate. On the other hand, Original UNIFAC and UNIFAC Dortmund resulted in less accurately predicted FP values in general in comparison to UNIFAC Bessa, except for the systems involving ethyl myristate for which UNIFAC Bessa's RMSDs are slightly higher.

A tendency previously observed for binary systems composed by saturated FAEEs was that the non-ideal character of the binary solution increases according to the difference between carbon chain sizes of the molecules involved in the mixture. This tendency is the same when it comes to systems of saturated + unsaturated FAEEs. We observed that the non-ideal character of the solution becomes more relevant when the difference in the carbon chain sizes of components increases. The FP prediction of a mixture of ethyl octanoate (C8:0), for example, with ethyl oleate (C18:1) can be significantly improved, in comparison to the ideal model result (RMSD of 2.95 K) by employing a UNIFAC type model, such as UNIFAC Bessa (RMSD of 1.02 K).

As Table 8 shows, UNIFAC Bessa resulted in better FP prediction in general, with a max. *RMSD* of 1.02 K in contrast with the *RMSD* of 3.78 K obtained for UNIFAC Dortmund. This is similar to what had been observed previously for saturated systems.

3.5. Flash point of biodiesel

FP values of four types of biodiesel from different feedstocks (corn, canola, cotton and soy oils) were measured in this study. Experimental FP values may be found in Table 9, while the characterization of each biodiesel is presented in Table 10. The characterization results through Gas Chromatography show that the major components in each biodiesel are ethyl palmitate (C16:0), ethyl stearate (C18:0), ethyl oleate (C18:1) and ethyl linoleate (C18:2). In terms of carbon chain size, there is not much difference between components, since the highest difference is by only two carbons between ethyl palmitate and the other compounds. This indicated that for these systems, a nearly ideal behavior could be expected.

Table 9
FP of biodiesel: predicted (Method 1) and experimental values.

Flash point of Biodiesel (K)					
Biodiesel	Experimental	Model			
		Ideal	UNIFAC	UNIFAC Dortmund	UNIFAC Bessa
Soy	456.5	454.9	454.8	454.9	454.3
Cotton	455.9	451.9	451.8	452.0	451.2
Corn	456.4	453.9	453.8	454.0	453.3
Canola	458.4	455.4	455.4	455.5	455.0

Table 10
Molar composition of biodiesel from fats and oils.

	Biodiesel			
FAEE	Soy	Cotton	Corn	Canola
ethyl palmitate	0.071	0.252	0.141	0.077
ethyl stearate	0.031	0.022	0.022	0.031
ethyl oleate	0.298	0.167	0.359	0.585
ethyl linoleate	0.599	0.559	0.478	0.307

Table 11
Average Absolute Deviation (AAD) between experimental and predicted values (Method 2) from the Ideal model and original UNIFAC, UNIFAC Dortmund and UNIFAC Bessa.

AAD (K)				
Biodiesel	Model			
	Ideal	UNIFAC	UNIFAC Dortmund	UNIFAC Bessa
soy	1.6	1.7	1.6	2.2
cotton	4.0	4.0	3.8	4.7
corn	2.5	2.6	2.4	3.1
canola	3.0	3.0	2.9	3.4
Max AAD (K)	4.0	4.0	3.8	4.7
Min AAD (K)	1.6	1.7	1.6	2.2

As foreseen, FP calculated from the Ideal model showed good agreement with experimental results. Out of the UNIFAC type models evaluated, UNIFAC – Dortmund was capable of slightly improving the FP prediction in comparison to the Ideal model, with a max AAD of 3.8 K and min AAD of 1.6 K (Table 11). However, the improvement observed was not significant (about 0.2 K). On the other hand, UNIFAC Bessa was not as accurate as the Ideal model or any of the other UNIFAC

type models.

This result was quite surprising due to the fact that UNIFAC Bessa parameters were adjusted specifically for biodiesel systems, and this model had previously provided accurate FP prediction for binary solutions involving both Unsaturated and Saturated FAEEs. In fact, the difference between UNIFAC Bessa's predictions in comparison to the other UNIFAC type models is lower than 0.9 K in the worst case scenario, which is not substantial.

There might be a few reasons as to why UNIFAC Bessa was not capable of improving FP prediction in this case. The main one is related to the characterization of the biodiesels. We did not consider trace amounts (lower than 1% m/m each) of other long chain esters on FP prediction calculations. Therefore, about 2% (m/m) of the composition of each biodiesel in terms of FAEEs was ignored in the calculations. Additionally, the presence of contaminants such as glycerol or ethanol or catalysts was not quantified. Any influence due to glycerol, a high FP contaminant, would not be substantial, although ethanol could affect biodiesel FP even in low concentrations [16]. As interactions between FAEEs tend to be mostly attractive, perhaps considering trace amounts of other esters could have changed the prediction results. In conclusion, we believe that the biodiesel representation in terms of only the four main components might have influenced the UNIFAC Bessa results.

4. Conclusions

This work presents experimental FP data of 9 pure FAEE, 20 FAEE binary systems, 2 FAEE ternary systems and Biodiesels from four different feedstocks (Canola, Corn, Cotton and Soy oils) measured in accordance with ASTM D6450 standard procedure. Liaw's model was employed to FP prediction for these systems in association with UNIFAC type models so that any possible liquid phase non-ideal behavior could be accounted for. Predicted FP values were compared to experimental values through RMSD and AAD calculation, showing that the UNIFAC Bessa based model is more accurate in FP prediction of saturated FAEE systems than any other studied model, with RMSDs varying from 0.27 to 2.18 K. However, the ideal model also results in comparably accurate FP prediction whenever carbon chains of individual compounds do not differ by more than 6 carbons in size. When there is a greater difference in carbon chain lengths between chemical species involved in the systems though, non-ideality description through activity coefficient models becomes important.

For Systems containing unsaturated FAEEs, UNIFAC Bessa shows the same accuracy in terms of FP prediction as previously noticed for most systems. Other UNIFAC type models are still able of improving the FP prediction in comparison to the ideal model for many of these systems, especially the binary ones containing ethyl laurate (C12:0) or ethyl myristate (C14:0) plus ethyl oleate (C18:1) or ethyl linoleate (C18:2). UNIFAC Bessa's accuracy in FP prediction of the binary systems is not reflected in the FP prediction of Biodiesels (Canola, Corn, Cotton and Soy oils) though. This could be due to the fact that long carbon chain FAEEs and possible other contaminants were ignored in FP prediction of these systems.

As Liaw's model requires not only liquid phase non-ideal behavior investigation, but also pure components vapor pressure estimation, the influence of the vapor pressure model selection was analyzed. Two vapor pressure models were compared for purely saturated systems: Antoine's model and a group contribution semi empirical method for fatty compounds. The results showed that there is no significant influence of the chosen option for FP prediction purposes, which means that both methods model fairly well the vapor pressure and can be used interchangeably for FP prediction of FAEE mixtures without loss of accuracy.

CRediT authorship contribution statement

Débora Costa do Nascimento: Software, Validation, Formal analysis, Writing - original draft, Visualization. **Natália Daniele Dorighello Carareto:** Investigation, Software, Validation, Formal analysis, Writing - original draft. **Antonio Marinho Barbosa Neto:** Supervision, Writing - review & editing. **Vincent Gerbaud:** Supervision, Writing - review & editing. **Mariana Conceição da Costa:** Project administration, Funding acquisition, Supervision, Writing - review & editing.

Declaration of Competing Interest

The authors declare that they have no known competing financial interests or personal relationships that could have appeared to influence the work reported in this paper.

Acknowledgments

We are grateful to CNPq (248539/2013-2, 310272/2017-3), FAPESP (2014/21252-0) and FAEPEX/UNICAMP for their financial support and assistantship. Additionally, this study was financed in part by the Coordenação de Aperfeiçoamento de Pessoal de Nível Superior – Brasil (CAPES) – Finance Code 001.

Appendix A. Supplementary data

Supplementary data to this article can be found online at https://doi.org/10.1016/j.fuel.2020.118717.

References

[1] Liaw HJ, Chiu YY. A general model for predicting the flash point of miscible mixtures. J Hazard Mater 2006;A137:38–46. https://doi.org/10.1016/j.jhazmat.2006.01.078.
[2] Liaw HJ, Chen CT, Cheng CC, Yang YT. Elimination of minimum flash-point behavior by addition of a specified third component. J Loss Prev Process Ind 2008. https://doi.org/10.1016/j.jlp.2007.10.001.
[3] Liaw HJ, Chen CT, Gerbaud V. Flash-point prediction for binary partially miscible aqueous-organic mixtures. Chem Eng Sci 2008;63:4543–54. https://doi.org/10.1016/j.ces.2008.06.005.
[4] Bagheri M, Borhani TNG, Zahedi G. Estimation of flash point and autoignition temperature of organic sulfur chemicals. Energy Convers Manag 2012. https://doi.org/10.1016/j.enconman.2012.01.014.
[5] Boog JHF, Silveira ELC, De Caland LB, Tubino M. Determining the residual alcohol in biodiesel through its flash point. Fuel 2011. https://doi.org/10.1016/j.fuel.2010.10.020.
[6] Černoch M, Hájek M, Skopal F. Relationships among flash point, carbon residue, viscosity and some impurities in biodiesel after ethanolysis of rapeseed oil. Bioresour Technol 2010. https://doi.org/10.1016/j.biortech.2010.05.003.
[7] Gharagheizi F, Alamdari RF. Prediction of flash point temperature of pure components using a Quantitative Structure-Property Relationship model. QSAR Comb Sci 2008;27:679–83. https://doi.org/10.1002/qsar.200730110.
[8] Gharagheizi F, Ilani-Kashkouli P, Farahani N, Mohammadi AH. Gene expression programming strategy for estimation of flash point temperature of non-electrolyte organic compounds. Fluid Phase Equilib 2012. https://doi.org/10.1016/j.fluid.2012.05.015.
[9] Katritzky AR, Stoyanova-Slavova IB, Dobchev DA, Karelson M. QSPR modeling of flash points: An update. J Mol Graph Model 2007. https://doi.org/10.1016/j.jmgm.2007.03.006.
[10] Saldana DA, Starck L, Mougin P, Rousseau B, Creton B. Prediction of flash points for fuel mixtures using machine learning and a novel equation. Energy Fuels 2013;27:3811–20. https://doi.org/10.1021/ef4005362.
[11] Wu Z, Zhou X, Liu X, Ni Y, Zhao K, Peng F, et al. Investigation on the dependence of flash point of diesel on the reduced pressure at high altitudes. Fuel 2016. https://doi.org/10.1016/j.fuel.2016.05.062.
[12] ASTM:D975-15b. Standard specification for diesel fuel oils. 2015. doi:10.1520/D0975-12A.2.
[13] ASTM D6751-15c. Standard specification for biodiesel fuel blend stock (B100) for middle distillate fuels. ASTM Int 2010. https://doi.org/10.1520/D6751.
[14] Moser BR. Biodiesel production, properties, and feedstocks. Vitr Cell Dev Biol – Plant 2009. https://doi.org/10.1007/s11627-009-9204-z.
[15] Bessa LCBA, Ferreira MC, Shiozawa S, Batista EAC, Meirelles AJA. Liquid + liquid equilibrium of systems involved in the stepwise ethanolysis of vegetable oils. J Chem Thermodyn 2015. https://doi.org/10.1016/j.jct.2015.04.036.
[16] Carareto NDD, Kimura CYCS, Oliveira EC, Costa MC, Meirelles AJA. Flash points of mixtures containing ethyl esters or ethylic biodiesel and ethanol. Fuel 2012;96:319–26. https://doi.org/10.1016/j.fuel.2012.01.025.
[17] Canapi E, Augustin Y, Moro E, Pedrosa E, Bendaño M. Coconut Oil. Baileys Ind. Oil

Fat Prod. John Wiley & Sons; 2005.
[18] Marlair G, Rotureau P, Breulet H, Brohez S. Booming development of biofuels for transport: Is fire safety of concern? Fire Mater 2009;33:1–19. https://doi.org/10.1002/fam.976.
[19] Casson Moreno V, Danzi E, Marmo L, Salzano E, Cozzani V. Major accident hazard in biodiesel production processes. Saf Sci 2019. https://doi.org/10.1016/j.ssci.2018.12.014.
[20] Calvo Olivares RD, Rivera SS, Núñez Mc Leod JE. Database for accidents and incidents in the biodiesel industry. J Loss Prev Process Ind 2014. https://doi.org/10.1016/j.jlp.2014.03.010.
[21] Hoshino T, Iwata Y, Koseki H. Oxidation stability and risk evaluation of biodiesel. Therm Sci 2007. https://doi.org/10.2298/TSCI0702087H.
[22] Zuleta EC, Baena L, Rios LA, Calderón JA. The oxidative stability of biodiesel and its impact on the deterioration of metallic and polymeric materials: a review. J Braz Chem Soc 2012. https://doi.org/10.1590/S0103-50532012001200004.
[23] Dantas MB, Albuquerque AR, Barros AK, Rodrigues Filho MG, Antoniosi Filho NR, Sinfrônio FSM, et al. Evaluation of the oxidative stability of corn biodiesel. Fuel 2011. https://doi.org/10.1016/j.fuel.2010.09.014.
[24] Demirbas A. Relationships derived from physical properties of vegetable oil and biodiesel fuels. Fuel 2008. https://doi.org/10.1016/j.fuel.2007.08.007.
[25] Ramadhas AS, Jayaraj S, Muraleedharan C. Biodiesel production from high FFA rubber seed oil. Fuel 2005. https://doi.org/10.1016/j.fuel.2004.09.016.
[26] Phoon LY, Hashim H, Mat R, Mustaffa AA. Flash point prediction of tailor-made green diesel blends containing B5 palm oil biodiesel and alcohol. Fuel 2016;175:287–93. https://doi.org/10.1016/j.fuel.2016.02.027.
[27] Álvarez A, Lapuerta M, Agudelo JR. Prediction of flash-point temperature of alcohol/biodiesel/diesel fuel blends. Ind Eng Chem Res 2019;58:6860–9. https://doi.org/10.1021/acs.iecr.9b00843.
[28] Dias RM, Aquino RT, Krähenbühl MA, Costa MC. Flash point of fatty acid methyl ester binary mixtures. J Chem Eng Data 2019;64:3465–72. https://doi.org/10.1021/acs.jced.9b00267.
[29] Paricaud P, Ndjaka A, Catoire L. Prediction of the flash points of multicomponent systems: applications to solvent blends, gasoline, diesel, biodiesels and jet fuels. Fuel 2019:263. https://doi.org/10.1016/j.fuel.2019.116534.
[30] Phoon LY, Mustaffa AA, Hashim H, Mat R. A review of flash point prediction models for flammable liquid mixtures. Ind Eng Chem Res 2014;53:12553–65. https://doi.org/10.1021/ie501233g.
[31] Sandler SI. Chemical and engineering thermodynamics. Book 1989.
[32] Gmehling J, Rasmussen P. Flash points of flammable liquid mixtures using UNIFAC. Ind Eng Chem Fundam 1982;21:186–8. https://doi.org/10.1021/i100006a016.
[33] Poling BE, Prausnitz JM, O'Connel JP. The properties of gases & liquids. 5th ed. McGraw-Hill Education; 2001. 10.1016/0894-1777(88)90021-0.
[34] Bessa LCBA, Ferreira MC, Abreu CRA, Batista EAC, Meirelles AJA. A new UNIFAC parameterization for the prediction of liquid-liquid equilibrium of biodiesel systems. Fluid Phase Equilib 2016. https://doi.org/10.1016/j.fluid.2016.05.020.
[35] Gmehling J, Lohmann J, Jakob A, Li J, Joh R. A modified UNIFAC (Dortmund) model. 3. Revision and extension. Ind Eng Chem Res 1998. https://doi.org/10.1021/ie980347z.
[36] Gmehling J, Li J, Schiller M. A modified UNIFAC Model 2. Present parameter matrix and results for different thermodynamic properties. Ind Eng Chem Res 1993. https://doi.org/10.1021/ie00013a024.
[37] Wu HS, Sandler SI. Use of ab initio quantum mechanics calculations in group contribution methods. 1. Theory and the basis for group identifications. Ind Eng Chem Res 1991. https://doi.org/10.1021/ie00053a010.
[38] Liaw HJ, Gerbaud V, Li YH. Prediction of miscible mixtures flash-point from UNIFAC group contribution methods. Fluid Phase Equilib 2011;300:70–82. https://doi.org/10.1016/j.fluid.2010.10.007.
[39] Liaw HJ, Gerbaud V, Wu HT. Flash-point measurements and modeling for ternary partially miscible aqueous-organic mixtures. J Chem Eng Data 2010. https://doi.org/10.1021/je100163q.
[40] Fredenslund A, Jones RL, Prausnitz JM. Group-contribution estimation of activity coefficients in nonideal liquid mixtures. AIChE J 1975;21:1086–99. https://doi.org/10.1002/aic.690210607.
[41] Weidlich U, Gmehling J. A modified UNIFAC model 1. Prediction of VLE, hE, and gamma∞. Ind Eng Chem Res 1987;26:1372–81. https://doi.org/10.1021/ie00067a018.
[42] Catoire L, Naudet V. A unique equation to estimate flash points of selected pure liquids application to the correction of probably erroneous flash point values. J Phys Chem Ref Data 2004;33:1083–111. https://doi.org/10.1063/1.1835321.
[43] Liaw HJ, Lee YH, Tang CL, Hsu HH, Liu JH. A mathematical model for predicting the flash point of binary solutions. J Loss Prev Process Ind 2002;15:429–38. https://doi.org/10.1016/S0950-4230(02)00068-2.
[44] Pan Y, Cheng J, Song X, Li G, Ding L, Jiang J. Flash points measurements and prediction for binary miscible mixtures. J Loss Prev Process Ind 2015. https://doi.org/10.1016/j.jlp.2015.01.022.
[45] Ceriani R, Gani R, Liu YA. Prediction of vapor pressure and heats of vaporization of edible oil/fat compounds by group contribution. Fluid Phase Equilib 2013;337:53–9. https://doi.org/10.1016/j.fluid.2012.09.039.
[46] Wang TY, Meng XZ, Jia M, Song XC. Predicting the vapor pressure of fatty acid esters in biodiesel by group contribution method. Fuel Process Technol 2015. https://doi.org/10.1016/j.fuproc.2014.11.030.
[47] Yuan W, Hansen AC, Zhang Q. Vapor pressure and normal boiling point predictions for pure methyl esters and biodiesel fuels. Fuel 2005. https://doi.org/10.1016/j.fuel.2005.01.007.
[48] Benziane M, Khimeche K, Mokbel I, Sawaya T, Dahmani A, Jose J. Experimental vapor pressures of five saturated fatty acid ethyl ester (FAEE) components of biodiesel. J Chem Eng Data 2011;56:4736–40. https://doi.org/10.1021/je200730m.
[49] Liaw HJ, Lu WH, Gerbaud V, Chen CC. Flash-point prediction for binary partially miscible mixtures of flammable solvents. J Hazard Mater 2008;153:1165–75. https://doi.org/10.1016/j.jhazmat.2007.09.078.
[50] Balasubramonian S, Srivastav RK, Kumar S, Sivakumar D, Sampath M, Kamachi Mudali U, et al. Flash point prediction for the binary mixture of phosphatic solvents and n-dodecane from UNIFAC group contribution model. J Loss Prev Process Ind 2015. https://doi.org/10.1016/j.jlp.2014.12.012.
[51] Catoire L, Paulmier S, Naudet V. Estimation of closed cup flash points of combustible solvent blends. J Phys Chem Ref Data 2006;35:9–14. https://doi.org/10.1063/1.1928236.
[52] Catoire L, Paulmier S, Naudet V. Experimental determination and estimation of closed cup flash points of mixtures of flammable solvents. Process Saf Prog 2006;25:33–9. https://doi.org/10.1002/prs.10112.
[53] Carareto NDD, Costa MC, Meirelles AJA, Pauly J. High pressure solid-liquid equilibrium of fatty acid ethyl esters binary systems. Fluid Phase Equilib 2014. https://doi.org/10.1016/j.fluid.2014.09.007.
[54] Zhang H, Yin Q, Liu Z, Gong J, Bao Y, Zhang M, et al. An odd-even effect on solubility of dicarboxylic acids in organic solvents. J Chem Thermodyn 2014. https://doi.org/10.1016/j.jct.2014.05.009.
[55] Gunstone FD. Fatty Acid and Lipid Chemistry. 1996. doi:10.1007/978-1-4615-4131-8.
[56] Metin S, Hartel RW. Crystallization of fats and oils. Bailey's Ind Oil Fat Prod 2005. https://doi.org/10.1002/047167849x.bio021.
[57] Products P, Principles S. Standard Test Method for Flash Point by Continuously Closed Cup (CCCFP) Tester 1. Annu B ASTM Stand 2011. doi:10.1520/D6450-05R10.Copyright.
[58] ASTM International. ASTM D93-18, Standard Test Methods for Flash Point by Pensky-Martens Closed Cup Tester 2018. doi:10.1520/D0093-18.

Supplementary Data

Flash point prediction with UNIFAC type models of ethylic biodiesel and binary/ ternary mixtures of FAEEs

*Débora Costa do Nascimento[a], Natália Daniele Dorighello Carareto[b], Antonio Marinho Barbosa Neto[c], Vincent Gerbaud[d] and Mariana Conceição da Costa[a]**

[a] School of Chemical Engineering (FEQ), University of Campinas (UNICAMP), 13083-852, Campinas, Sao Paulo, Brazil.

[b] Laboratoire des Matériaux Céramiques et Procédés Associés (LMCPA), Université de Valenciennes et du Hainaut-Cambrésis, Valenciennes, France.

[c] ThermoPhase, Department of Petroleum Engineering, Santa Catarina State University, 88336-275, Balneário Camboriú, Santa Catarina, Brazil.

[d] Laboratoire de Génie Chimique, Université de Toulouse, CNRS – INP – UPS, Toulouse, France.

* CORRESPONDING AUTHOR: Tel.:+55 19 3521 3962; E-mail address: mcdcosta@unicamp.br (M. C. Costa).

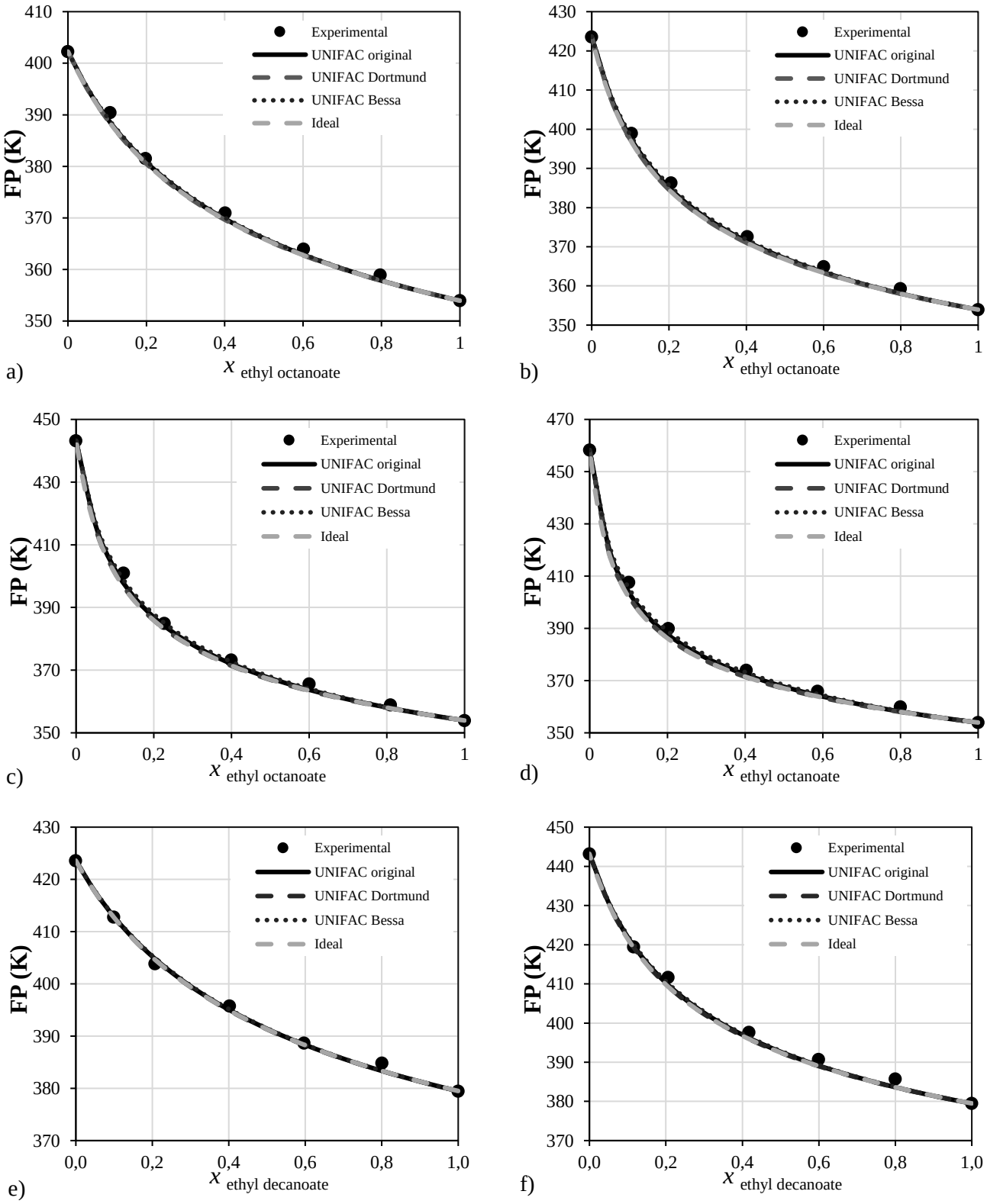

Fig. S1. Experimental and calculated flash point (with vapor pressure calculated using the Method 1) for the binary systems of: a) ethyl octanoate + ethyl laurate; b) ethyl octanoate + ethyl myristate; c) ethyl octanoate + ethyl palmitate; d) ethyl octanoate + ethyl stearate; e) ethyl decanoate + ethyl myristate and; f) ethyl decanoate + ethyl palmitate.

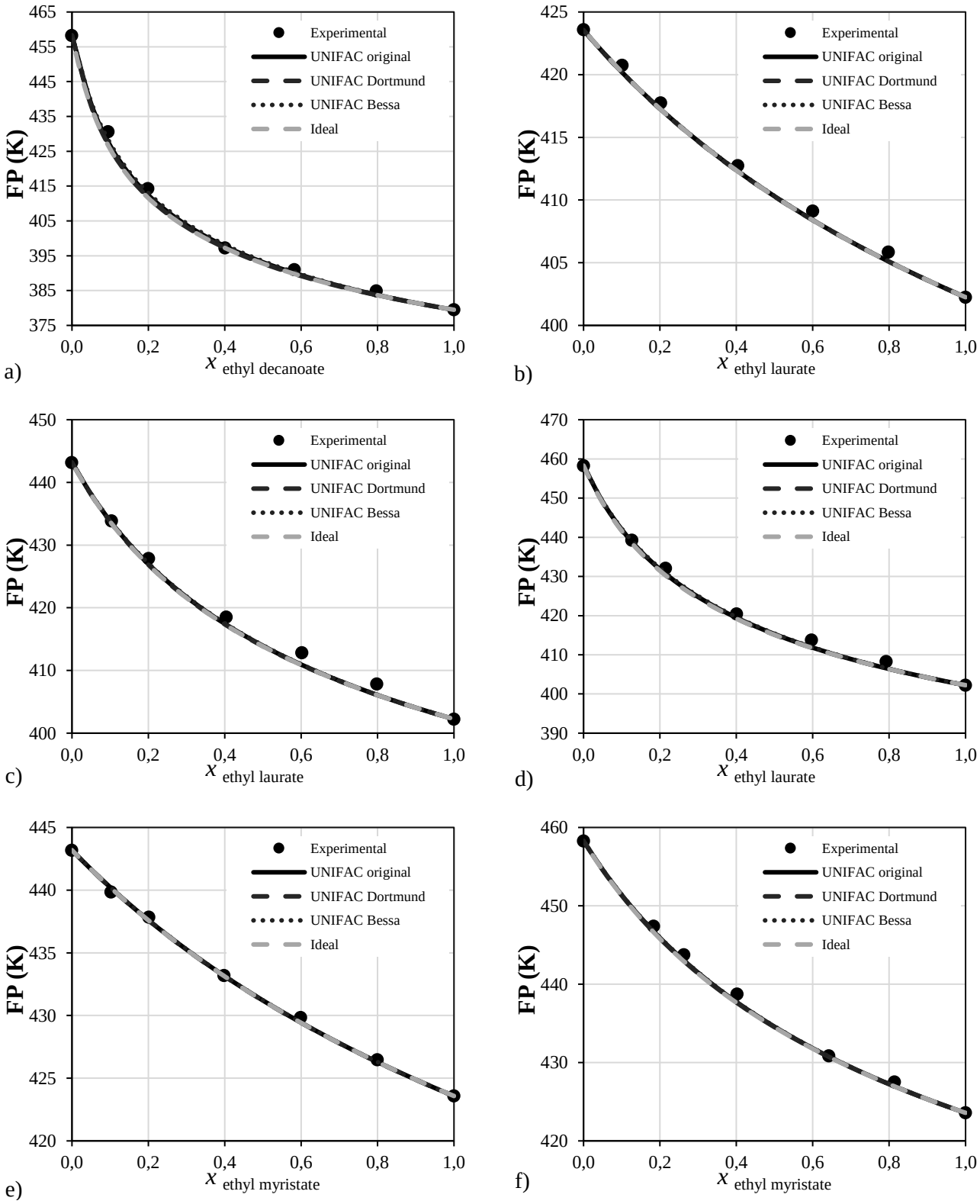

Fig. S2. Experimental and calculated flash point (with vapor pressure calculated using the Method 1) for the binary systems of: a) ethyl decanoate + ethyl stearate; b) ethyl laurate + ethyl myristate; c) ethyl laurate + ethyl palmitate; d) ethyl laurate + ethyl stearate; e) ethyl myristate + ethyl palmitate and; f) ethyl myristate + ethyl stearate.

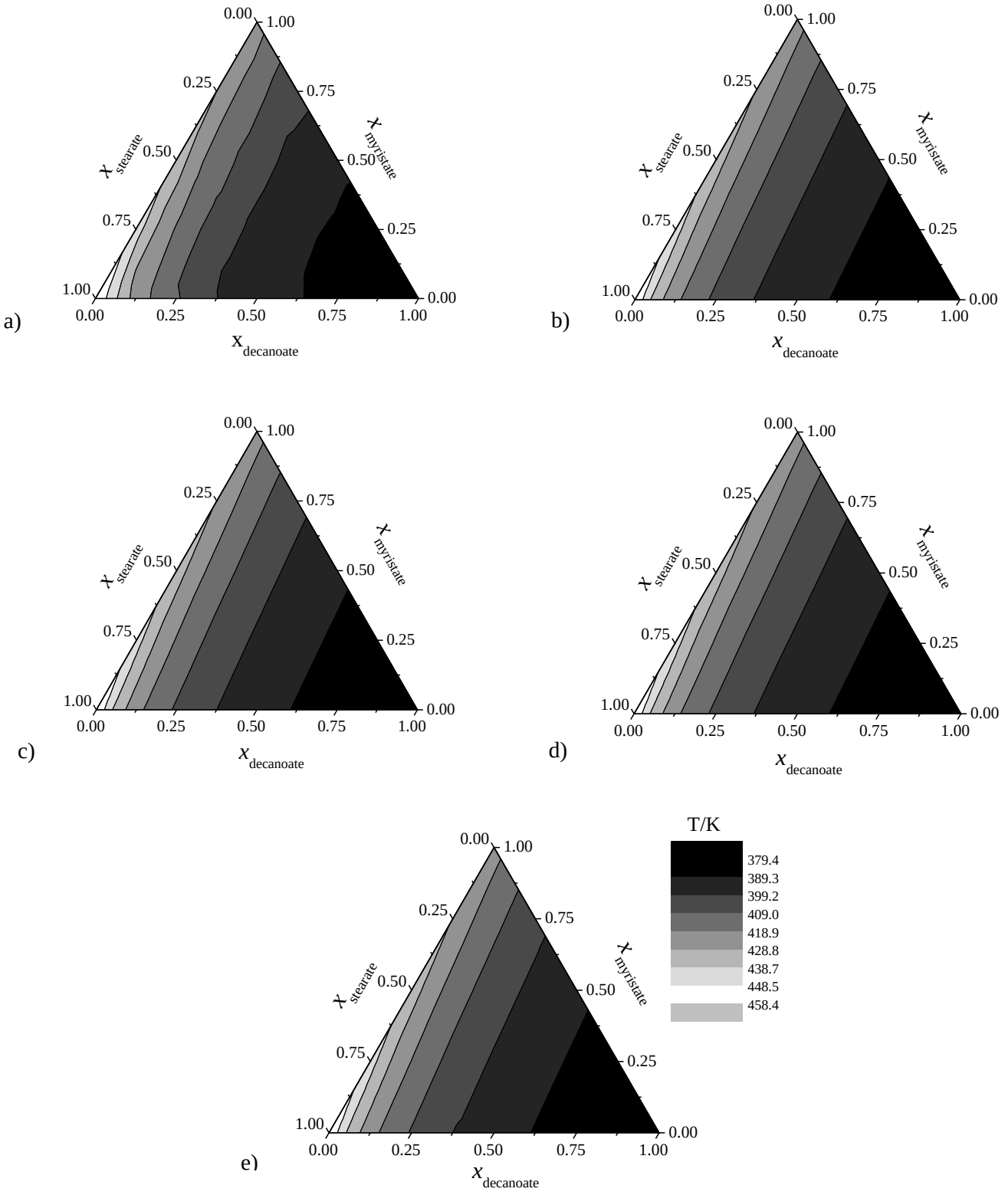

Fig. S3. Experimental and calculated flash point (with vapor pressure calculated using the Method 1) for the ethyl decanoate + ethyl myristate + ethyl stearate ternary system. a) experimental; b) ideal; c) UNIFAC original; d) UNIFAC Dortmund and; e) UNIFAC Bessa.

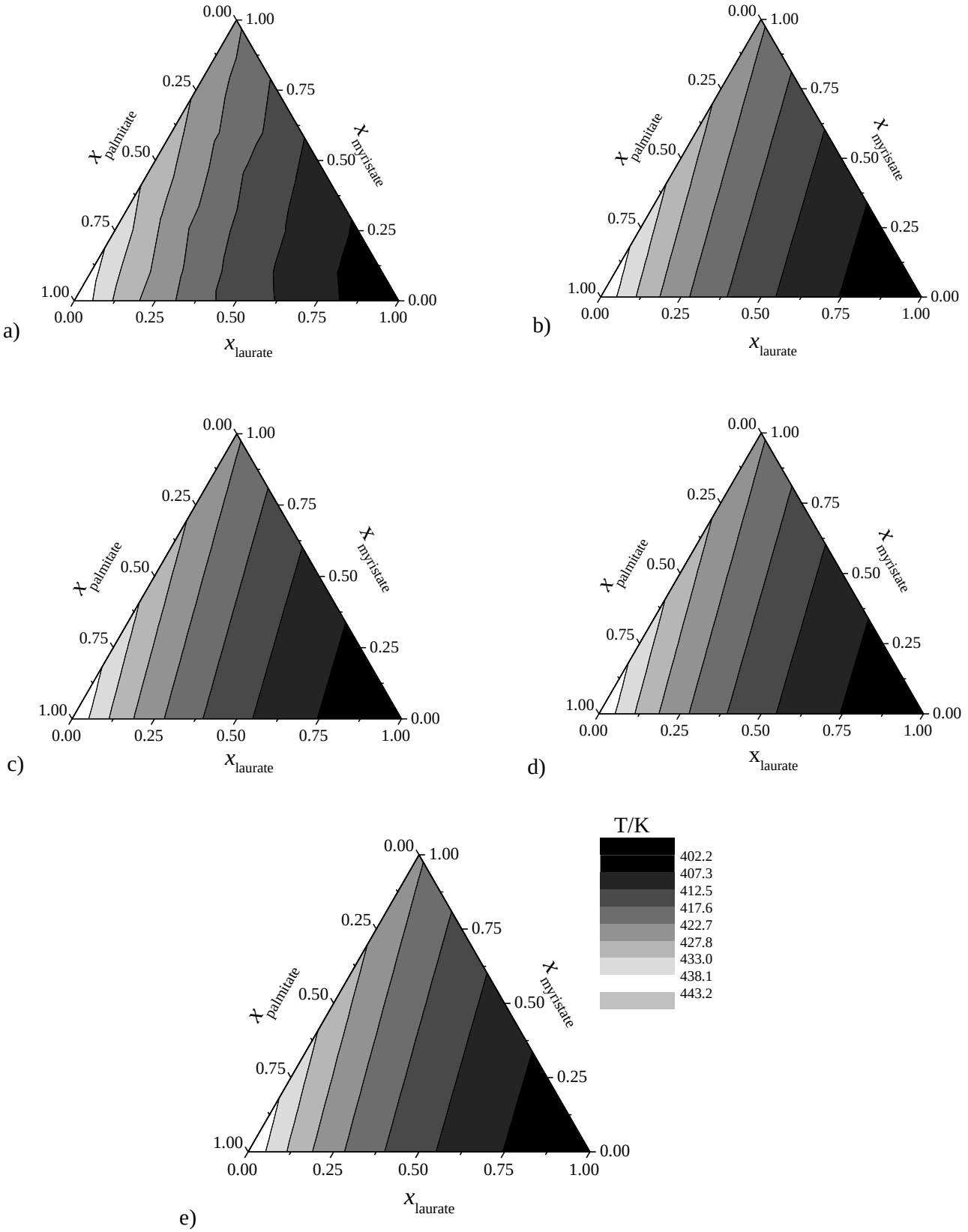

Fig. S4. Experimental and calculated flash point (with vapor pressure calculated using the Method 1) for the ethyl laurate + ethyl myristate + ethyl palmitate ternary system. a) experimental; b) ideal; c) UNIFAC original; d) UNIFAC Dortmund and; e) UNIFAC Bessa.

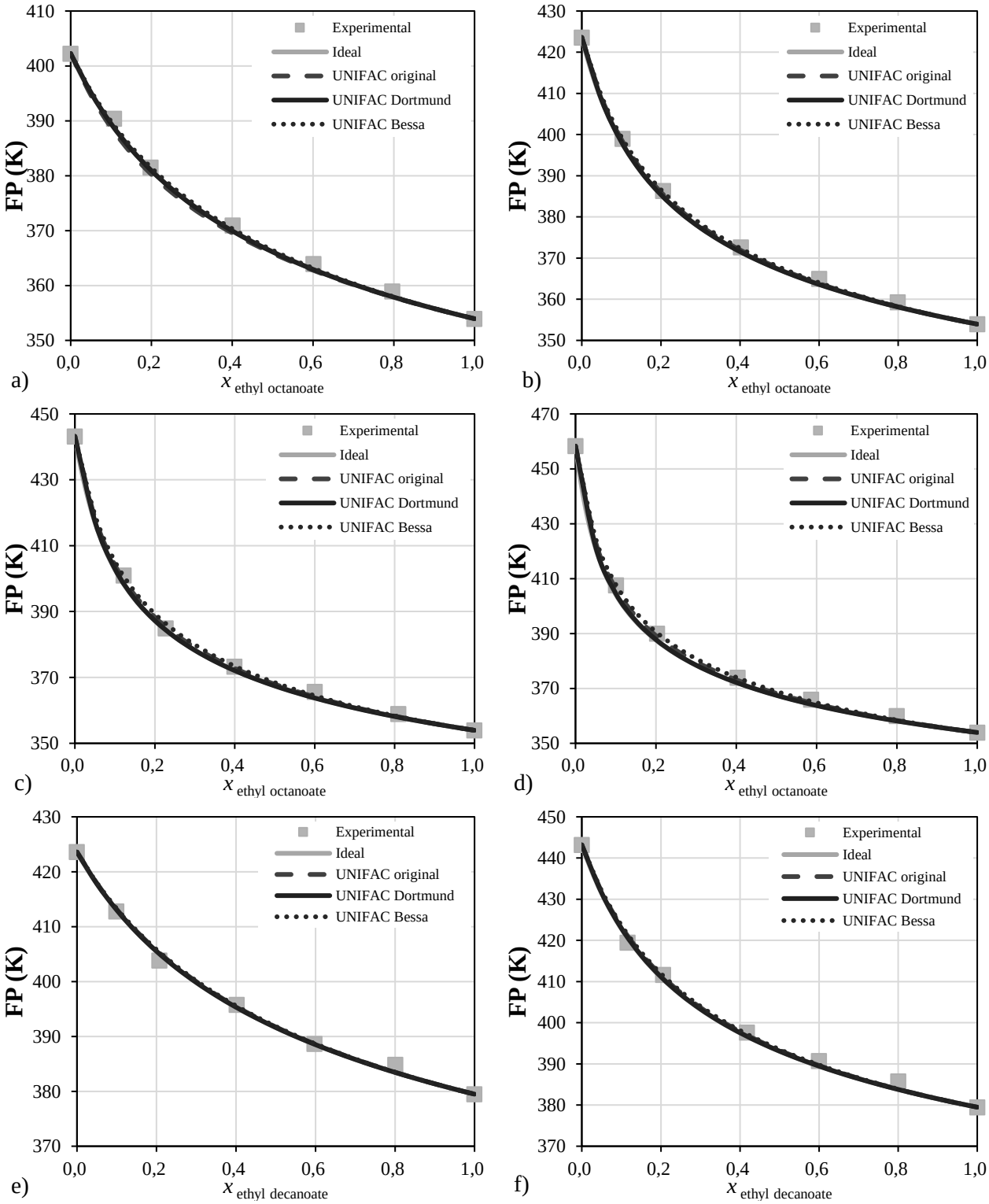

Fig. S5. Experimental and calculated flash point (with vapor pressure calculated using the Method 2) for the binary systems of: a) ethyl octanoate + ethyl laurate; b) ethyl octanoate + ethyl myristate; c) ethyl octanoate + ethyl palmitate; d) ethyl octanoate + ethyl stearate; e) ethyl decanoate + ethyl myristate and; f) ethyl decanoate + ethyl palmitate.

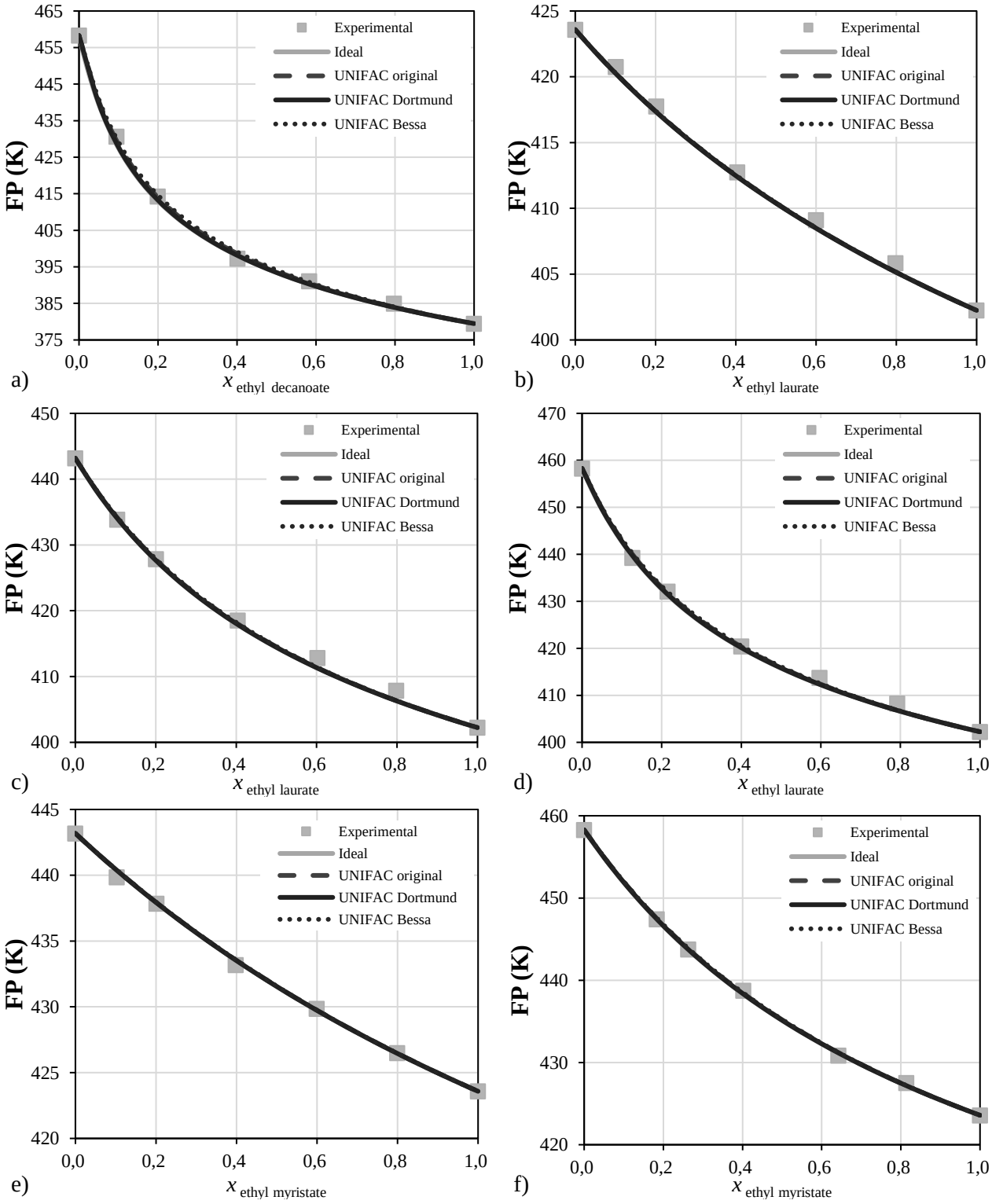

Fig. S6. Experimental and calculated flash point (with vapor pressure calculated using the Method 2) for the binary systems of: a) ethyl decanoate + ethyl stearate; b) ethyl laurate + ethyl myristate; c) ethyl laurate + ethyl palmitate; d) ethyl laurate + ethyl stearate; e) ethyl myristate + ethyl palmitate and; f) ethyl myristate + ethyl stearate.

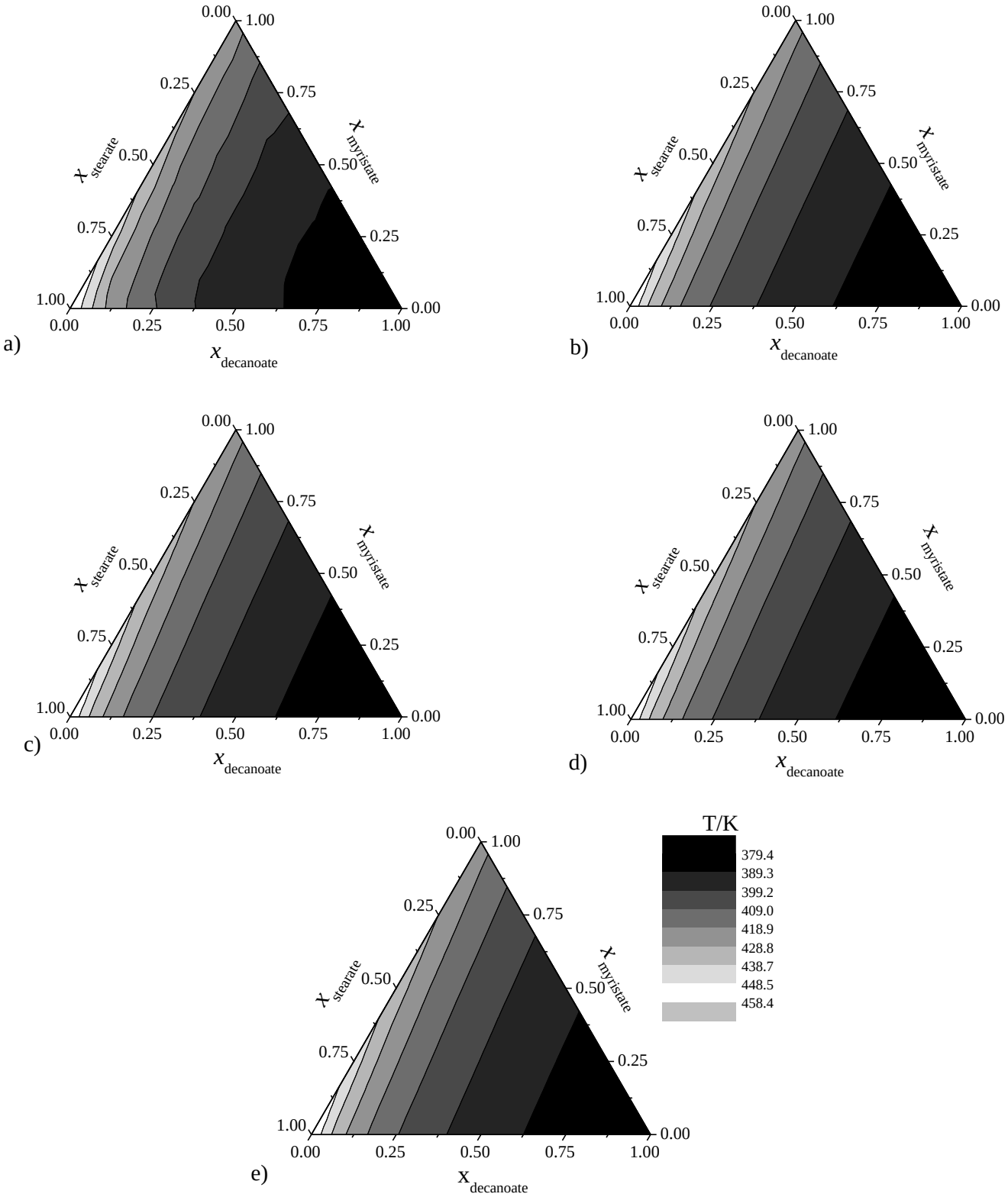

Fig. S7. Experimental and calculated flash point (with vapor pressure calculated using the Method 2) for the ethyl decanoate + ethyl myristate + ethyl stearate ternary system. a) experimental; b) ideal; c) UNIFAC original; d) UNIFAC Dortmund and; e) UNIFAC Bessa.

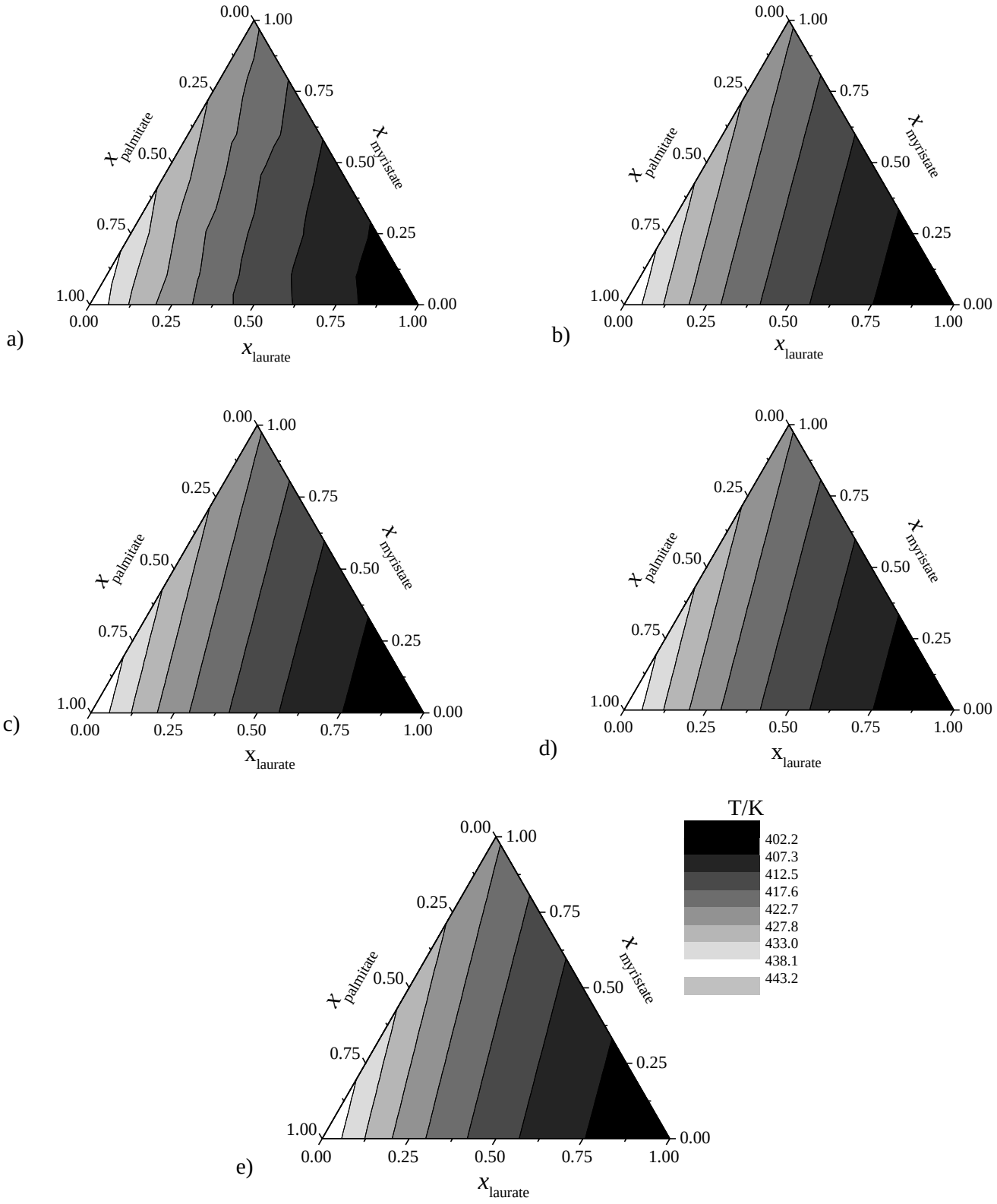

Fig. S8. Experimental and calculated flash point (with vapor pressure calculated using the Method 2) for the ethyl laurate + ethyl myristate + ethyl palmitate ternary system. a) experimental; b) ideal; c) UNIFAC original; d) UNIFAC Dortmund and; e) UNIFAC Bessa.

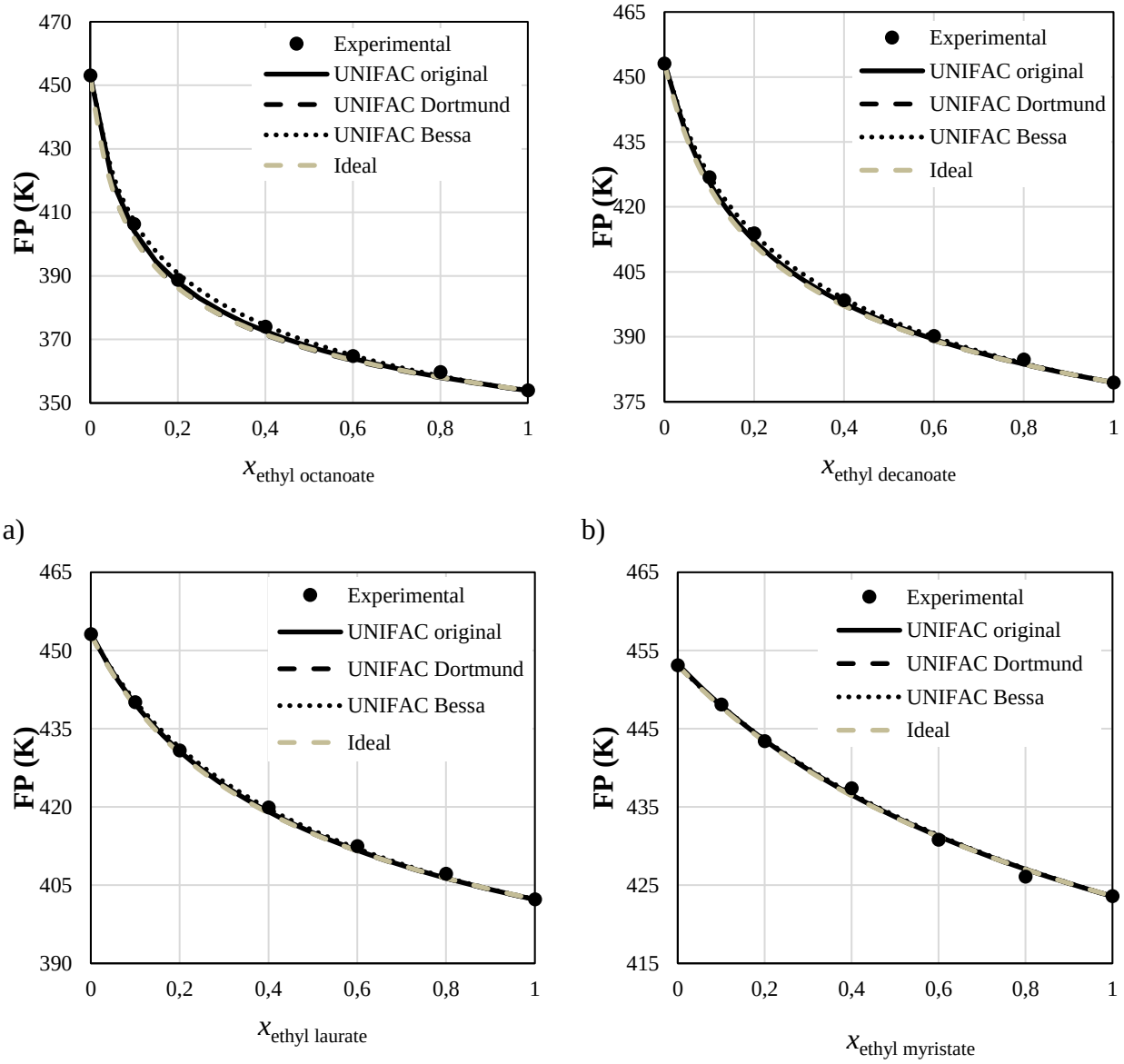

Fig S9. Experimental and calculated flash point (with vapor pressure calculated using the Method 1) for the binary systems of: a) ethyl octanoate + ethyl oleate; b) ethyl decanoate + ethyl oleate; c) ethyl laurate + ethyl oleate; d) ethyl myristate + ethyl oleate.

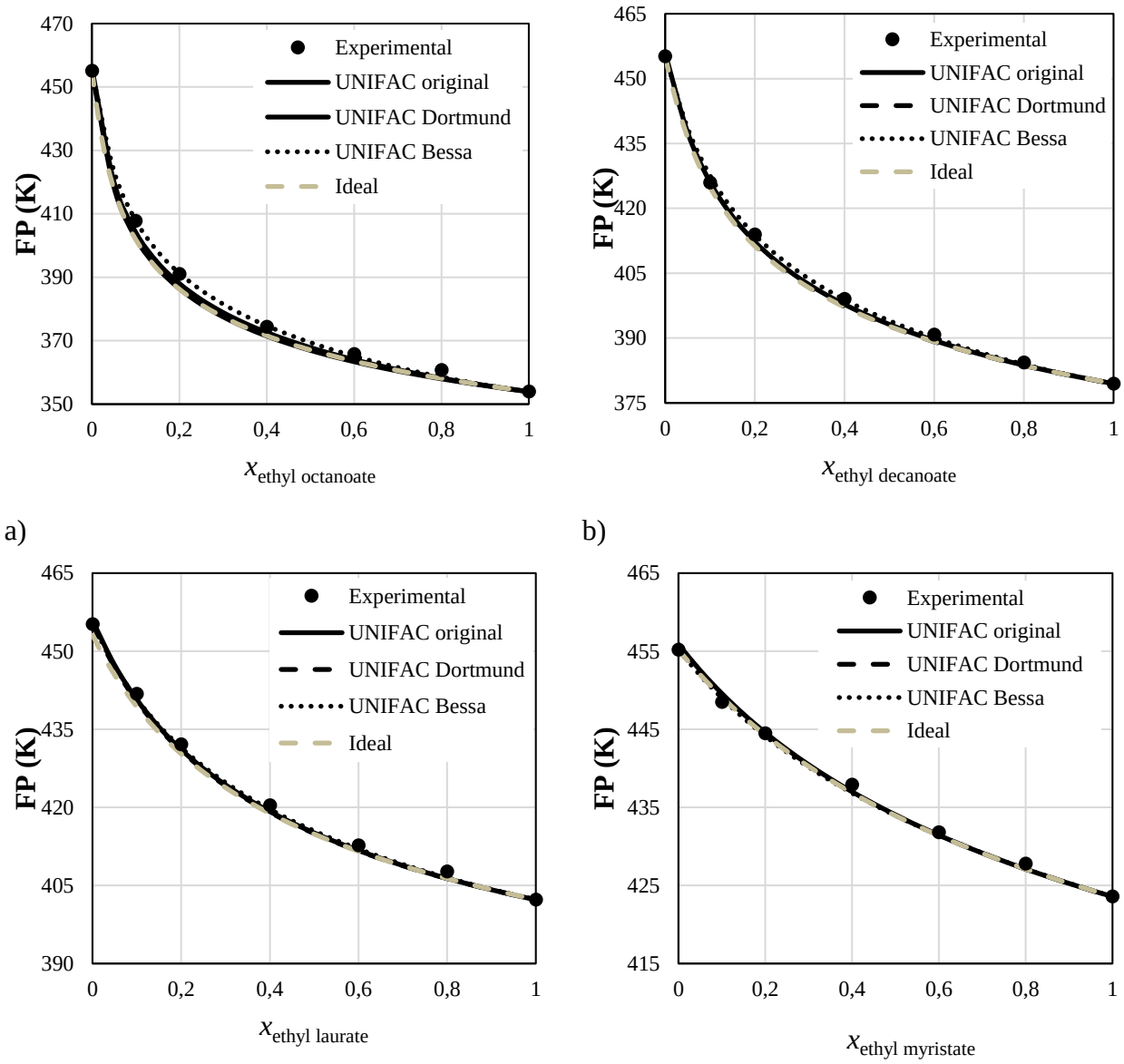

Fig S10. Experimental and calculated flash point (with vapor pressure calculated using the Method 1) for the binary systems of: a) ethyl octanoate + ethyl linoleate; b) ethyl decanoate + ethyl linoleate; c) ethyl laurate + ethyl linoleate; d) ethyl myristate + ethyl linoleate.

Table S1. Normal boiling points (T_b) and number of carbons of FAEEs.

FAEE	T_b (K)	n
ethyl octanoate (106-32-1)	479.64[a]	10
ethyl decanoate (110-38-3)	515.95[a]	12
ethyl laurate (106-33-2)	547.48[a]	14
ethyl myristate (124-06-1)	581.95[a]	16
ethyl palmitate (628-97-7)	607.15[b]	18
ethyl stearate (111-61-5)	629.15[b]	20
ethyl oleate (111-62-6)	630.15[b]	20
ethyl linoleate (544-35-4)	624.15[b]	20

[a]apud [1]

[b]apud [2]

References:

[1] Evangelista NS, Do Carmo FR, De Sant'Ana HB. Estimation of Vapor Pressures and Enthalpies of Vaporization of Biodiesel-Related Fatty Acid Alkyl Esters. Part 1. Evaluation of Group Contribution and Corresponding States Methods. Ind Eng Chem Res 2017. doi:10.1021/acs.iecr.6b04772.

[2] Heynes WM, Lide DR, Bruno TJ, editors. CRC Handbook of Chemistry and Physics. 95th ed. CRC Press. Taylor and Francis Group; n.d.